This article has been accepted for publication in a future issue of this journal, but has not been fully edited. Content may change prior to final publication. Citation information: DOI 10.1109/TSP.2014.2307835, IEEE Transactions on Signal Processing

Noncooperative Day-Ahead Bidding Strategies for Demand-Side Expected Cost Minimization with Real-Time Adjustments: A GNEP Approach

Italo Atzeni, Luis G. Ordóñez, Gesualdo Scutari, Daniel P. Palomar, and Javier R. Fonollosa

***Abstract*—The envisioned smart grid aims at improving the interaction between the supply- and the demand-side of the electricity network, creating unprecedented possibilities for optimizing the energy usage at different levels of the grid. In this paper, we propose a distributed demand-side management (DSM) method intended for smart grid users with load prediction capabilities, who possibly employ dispatchable energy generation and storage devices. These users participate in the day-ahead market and are interested in deriving the bidding, production, and storage strategies that jointly minimize their expected monetary expense. The resulting day-ahead grid optimization is formulated as a generalized Nash equilibrium problem (GNEP), which includes global constraints that couple the users' strategies. Building on the theory of variational inequalities, we study the main properties of the GNEP and devise a distributed, iterative algorithm converging to the variational solutions of the GNEP. Additionally, users can exploit the reduced uncertainty about their energy consumption and renewable generation at the time of dispatch. We thus present a complementary DSM procedure that allows them to perform some unilateral adjustments on their generation and storage strategies so as to reduce the impact of their real-time deviations with respect to the amount of energy negotiated in the day-ahead. Finally, numerical results in realistic scenarios are reported to corroborate the proposed DSM technique.**

***Index Terms*—Game Theory, Generalized Nash Equilibrium Problem, Variational Inequality, Proximal Decomposition Algorithm, Smart Grid, Day-Ahead/Real-Time Demand-Side Management.**

I. Introduction

The electricity distribution infrastructure is facing a profound transformation with the development of the smart grid concept, which improves the interaction between the supply- and the demand-side of the network by means of demand-side management (DSM) techniques. Indeed, taking advantage of information and communication technologies, DSM methods introduce advanced mechanisms for encouraging the demand-side to participate actively in the network optimization process [1]. Furthermore, DSM, properly integrated with distributed energy generation (DG) and distributed storage (DS), is considered an increasingly essential element for implementing the smart grid paradigm and balancing massive energy production from renewable sources. These concepts allow for an immense opportunity for optimizing the energy grid and energy usage at different levels of the network.

The short-term electricity market[1] consists mainly of a day-ahead market, which produces financially binding schedules for energy supply and demand before the operating day, and a real-time market, used to balance day-ahead and real-time energy requirements [2, Ch. 1.2]. In line with the time granularity of the energy trading process, day-ahead and real-time DSM methods are successfully employed in a complementary fashion in practical situations [3]. In particular, a day-ahead demand-side optimization allows energy users to efficiently manage their electricity consumption and provides the supply-side with an estimation of the amount of energy to be delivered over the upcoming day, so that the production can be planned accordingly [4]. Nonetheless, when the consumption schedule is not correctly predicted by the users, the supply-side incurs additional costs that are transferred to the demand-side in the form of penalty charges [5], [6]. On the other hand, real-time DSM techniques bring the grid optimization process to a finer time scale, allowing to take into consideration possible contingencies in the supply-side and reducing the uncertainties induced by the renewable energy sources and by the randomness of the users' consumption (see, e.g., [7], [8]).

A common DSM procedure is energy consumption scheduling (ECS) [9], [10], [11], which modifies the demand profile by shifting flexible energy consumption to off-peak hours. The implementation of ECS techniques has been shown to be successful in diminishing the peak-to-average ratio (PAR) of the energy demand curve, from which both demand- and supply-side benefit in terms of reduced energy cost, CO_2 emissions, and overall power plants requirements [12]. However, since the users' inconvenience must be taken into account (e.g., the rescheduling of activities results in lost services for industrial customers [13]), ECS presents flexibility limitations that can be overcome by incorporating dispatchable DG and DS into the demand-side of the network. The combined day-ahead optimization of dispatchable DG and DS has been studied in [14], [15] assuming deterministic consumption profiles.

The work of Italo Atzeni, Luis G. Ordóñez, and Javier R. Fonollosa was supported in part by the Spanish Ministry of Economy and Competitiveness (CONSOLIDER CSD2008-00010 COMONSENS, and TEC2010-19171 MOSAIC) and by the Catalan Government (2009 SGR-01236 AGAUR). The work of Gesualdo Scutari was supported by the USA National Science Foundation under Grants CMS 1218717 and CAREER Award No. 1254739. The work of Daniel P. Palomar was supported by the Hong Kong RGC 617911 research grant.

I. Atzeni, L. G. Ordóñez, and J. R. Fonollosa are with the Signal Processing and Communications Group, Universitat Politècnica de Catalunya – Barcelona Tech, 08034 Spain (email: italo.atzeni@upc.edu; luis.g.ordonez@upc.edu; javier.fonollosa@upc.edu).

G. Scutari is with the Department of Electrical Engineering, University at Buffalo, the State University of New York (SUNY), Buffalo, NY 14260, USA (email: gesualdo@buffalo.edu).

D. P. Palomar is with the Department of Electric and Computer Engineering, Hong Kong University of Science and Technology (HKUST), Clear Water Bay, Kowloon, Hong Kong (email: palomar@ust.hk).

[1]Medium- and long-term electricity trading between producers and retailers/consumers, which take place through futures markets and bilateral contracts [2, Ch. 1.2], are not the focus of the present paper.

This article has been accepted for publication in a future issue of this journal, but has not been fully edited. Content may change prior to final publication. Citation information: DOI 10.1109/TSP.2014.2307835, IEEE Transactions on Signal Processing

However, this approach cannot accommodate potential real-time deviations from the users' expected energy consumption, neither the randomness of their renewable sources.

Additionally, to achieve a realistic smart grid model, some global requirements, e.g., lower and upper bounds on the aggregate load at specific time intervals [16], must be imposed to comply with the physical constraints of both the supply and the power grid. Besides, the energy price curve, derived by combining the production offers of the individual energy generators in the supply-side of the network, is only valid within a certain range. These limits can be also established so as to force the desired shaping of the aggregate load, e.g., in order to reduce the PAR. By all means, such global constraints result in a coupling between the strategies of the users that has not been addressed in the literature yet.

The main contribution of this paper is to fill the gap in considering the above global grid requirements and to propose a novel DSM method that consists in a day-ahead optimization in the presence of coupling constraints among smart grid users, followed by a real-time optimization. More specifically, the DSM is carried out through (see Fig. 2): i) a day-ahead bidding process where demand-side users with DG, DS, and additional load prediction capabilities minimize their expected monetary expense in a competitive market environment; ii) successive real-time adjustments of the generation and storage strategies that exploit the reduced uncertainty about the users' energy consumption at the time of dispatch.

During the day-ahead bidding process, the subscribers' consumption and renewable generation are still uncertain: these quantities are thus modeled as random variables. Based on the corresponding probability distributions, the users individually calculate their bidding, dispatchable production, and storage strategies in a distributed fashion with the objective of minimizing their expected monetary expense. Given the selfish nature of the users and the global requirements on their aggregate load, we formulate the bidding process as a generalized Nash equilibrium problem (GNEP) [17].[2] Building on the variational inequality (VI) framework [17], [19], [20], we analyze the existence of variational solutions of the GNEP. However, the coupling constraints prevent the application of well-known game theoretical decomposition methods, making the design of distributed algorithms a difficult task. In order to deal with the coupling in a distributed way, we propose a pricing-based, iterative scheme that converges to the variational solutions under some technical conditions. Indeed, this paper is the first attempt towards the solution of such a problem in the smart grid literature. Interestingly, we also show that the proposed framework can be easily adapted to incorporate ECS to the optimization of the bidding strategies.

Once the day-ahead bidding process has taken place, and as the dispatch time approaches, users gain a better knowledge about their energy needs and renewable generation. Based on this coming information, we also devise a real-time method for repeatedly recalculating the production and storage strategies throughout the day period to alleviate the impact of real-time deviations with respect to their day-ahead bid loads.

The problem of deriving the optimal bidding strategies of energy generators and retailers in the sequence of different trading markets has been addressed in a number of works in the power systems literature (a good summary is given in [21]). In such context, the involved agents determine the most profitable combination of buying/selling offers, while dealing with the uncertainty associated with the forecast energy prices [16]. The present paper tackles a substantially different problem: under the smart grid paradigm, energy prices directly depend on the demand-side users' strategies and, therefore, our stochastic formulation rather refers to the uncertainty induced by the end users' energy consumption and renewable generation.

The rest of the paper is structured as follows. Sections II and III introduce the overall smart grid framework and the proposed DSM method. Section IV describes the day-ahead DSM approach with coupled strategies of the users. Section V presents a real-time procedure to adjust the users' production and storage strategies. Section VI illustrates the proposed methods and algorithms through experimental evaluations and comparisons with ECS approaches. Finally, we provide some conclusions in Section VII.

Notation. The following notation is used throughout the paper. Lowercase and uppercase boldface denote vectors and matrices, respectively. The operator $\succ$ ($\succeq$) for vectors is defined componentwise, while for matrices it refers to the positive (semi) definiteness property. The matrix $\mathbf{I}_a$ is the a-dimensional identity matrix, while $\mathbf{0}$ is the zero vector. By (a, b) we denote the vertical concatenation of the scalar or vector arguments a and b, $\left(x_a\right)_{a=1}^{A}$ represents the vertical concatenation of scalar or vector arguments x_a ordered according to the index a, and $\{x_a\}_{a\in\mathcal{A}}$ indicates the set of elements x_a with indices $a \in \mathcal{A}$. The operator $\mathrm{Diag}(\cdot)$ results in a diagonal matrix with elements given by the the vector argument or in a block-diagonal of the matrix arguments, whereas $\otimes$ denotes the Kronecker product. Lastly, the operator $(\cdot)^+ \triangleq \max(\cdot, 0)$ extracts the positive part of the scalar argument.

II. Smart Grid Model

The modern power grid is a complex network that can be conveniently divided into [8], [22]: i) supply-side (energy producers and providers); ii) central unit (regulation authority that coordinates the proposed demand-side bidding process); iii) demand-side (end users). In this paper, we focus our attention on the demand-side of the smart grid, which is introduced in Section II-A and further refined in Sections II-B and III-A, whereas the supply-side and the central unit are modeled as simply as possible.

A. Demand-Side Model

Demand-side users, whose associated set is denoted by $\mathcal{D}$, are characterized in the first place by the individual *per-slot net energy consumption* $e_n(h)$ indicating the energy needed by user $n \in \mathcal{D}$ to supply his appliances at time-slot h in the time period of analysis, which corresponds to a day. This term also accounts for eventual non-dispatchable (renewable)

[2] A cooperative method applied to the same framework and that neglects the coupling constraints has been addressed in [18].

This article has been accepted for publication in a future issue of this journal, but has not been fully edited. Content may change prior to final publication. Citation information: DOI 10.1109/TSP.2014.2307835, IEEE Transactions on Signal Processing

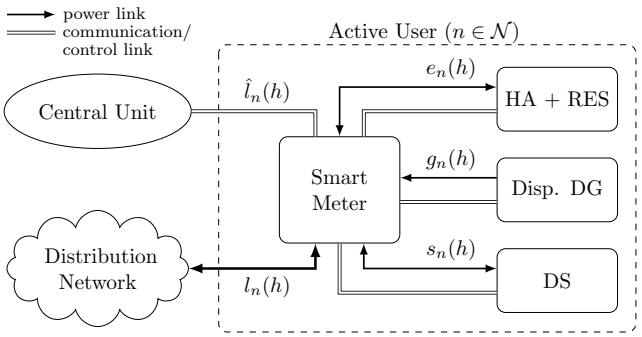

Fig. 1. Connection scheme between the smart grid and one active user consisting of: home appliances (HA), renewable energy source (RES), dispatchable distributed generation (DG) and distributed storage (DS).

energy resources that the user may have.[3] In order to tackle with the uncertainties related to the future load demands and to the renewable sources, $e_n(h)$ is modeled as a random variable with pdf $f_{e_n(h)}(\cdot)$ and cdf $F_{e_n(h)}(\cdot)$.

Our model distinguishes between *passive* and *active* users. Passive users are basically energy consumers and resemble traditional demand-side users, whereas active users indicate those consumers participating in the demand-side bidding process, i.e., reacting to changes in the cost per unit of energy by modifying their day-ahead bidding strategies. For convenience, we group the P passive users into the set $\mathcal{P} \subset \mathcal{D}$ and the N active users into the set $\mathcal{N} \triangleq \mathcal{D} \backslash \mathcal{P}$. We suppose that each active user can derive his individual load and renewable production statistics from his energy consumption history and data measurements, i.e., we suppose that $f_{e_n(h)}(\cdot)$ and $F_{e_n(h)}(\cdot)$ are known. Furthermore, in order to participate in the optimization process, active users are connected not only to the power distribution grid, but also to a communication infrastructure that enables bidirectional communication between their smart meter and the central unit [1] (see Fig. 1). Lastly, we conveniently divide the day period into H time-slots.

B. Energy Generation and Storage Model

Let us use $\mathcal{G} \subseteq \mathcal{N}$ to denote the subset of users possessing dispatchable DG (e.g., internal combustion engines, gas turbines, or fuel cells). For users $n \in \mathcal{G}$, $g_n(h) \geq 0$ represents the *per-slot energy production profile* at time-slot h. Introducing the *energy production scheduling vector* $\mathbf{g}_n \triangleq \big(g_n(h)\big)_{h=1}^{H}$, we have that $\mathbf{g}_n \in \Omega_{\mathbf{g}_n}$, where $\Omega_{\mathbf{g}_n}$ is the strategy set for dispatchable energy producer $n \in \mathcal{G}$ (see Section VI). Moreover, the *production cost function* $W_n\big(g_n(h)\big)$ gives the variable production costs (e.g., the fuel costs) incurred by user $n \in \mathcal{G}$ for generating the amount of energy $g_n(h)$ at time-slot h, with $W_n(0) = 0$.

Likewise, we use $\mathcal{S} \subseteq \mathcal{N}$ to denote the subset of users owning DS devices. Users $n \in \mathcal{S}$ are characterized by the *per-slot energy storage profile* $s_n(h)$ at time-slot h: we have $s_n(h) > 0$ when the storage device is to be charged, $s_n(h) < 0$ when the storage device is to be discharged, and $s_n(h) = 0$ when the device is inactive. Introducing the *energy storage scheduling vector* $\mathbf{s}_n \triangleq \big(s_n(h)\big)_{h=1}^{H}$, it holds that $\mathbf{s}_n \in \Omega_{\mathbf{s}_n}$, being $\Omega_{\mathbf{s}_n}$ the strategy set for energy storer $n \in \mathcal{S}$ (see Section VI).[4]

Let us now introduce the individual *per-slot energy load*

$$l_n(h) \triangleq e_n(h) - g_n(h) + s_n(h) \tag{1}$$

which gives the real-time energy flow between user $n \in \mathcal{N}$ and the grid at time-slot h, with $l_n(h) > 0$ when user n purchases energy from the grid and $l_n(h) < 0$ when user n sells energy to the grid, as shown schematically in Fig. 1.

III. DSM Model

We are now ready to introduce the proposed demand-side optimization model along with the DSM approach by which active users determine their bidding, production, and storage strategies at two different time granularities (see Fig. 2). The procedure described in the following is consistent with the actual functioning of electricity markets (see, e.g., [2, Ch. 1] for more details) allowing multi-round auctions [23].

A. Energy Load Bidding Model

Let us denote by $\tilde{e}_n(h)$ the *per-slot bid net energy consumption*, i.e., the day-ahead amount of energy (to be optimized) that user $n \in \mathcal{N}$ commits to consume at time-slot h. The corresponding *bidding strategy vector* is $\tilde{\mathbf{e}}_n \triangleq \big(\tilde{e}_n(h)\big)_{h=1}^{H}$, and the bidding strategy set $\Omega_{\tilde{\mathbf{e}}_n}$ can be expressed as

$$\Omega_{\tilde{\mathbf{e}}_n} \triangleq \big\{\tilde{\mathbf{e}}_n \in \mathbb{R}^H : \chi_n^{(\min)}(h) \leq \tilde{e}_n(h) \leq \chi_n^{(\max)}(h), \forall h\big\} \tag{2}$$

with $\chi_n^{(\min)}(h)$ and $\chi_n^{(\max)}(h)$ denoting the minimum and maximum per-slot bidding consumption, respectively.

Let us define the *per-slot bid energy load* of user $n \in \mathcal{N}$ as

$$\tilde{l}_n(h) \triangleq \tilde{e}_n(h) - g_n(h) + s_n(h) \tag{3}$$

and the strategy vector as $\mathbf{x}_n \triangleq \big(\mathbf{x}_n(h)\big)_{h=1}^{H}$, with

$$\mathbf{x}_n(h) \triangleq \big(\tilde{e}_n(h), g_n(h), s_n(h)\big). \tag{4}$$

Taking into account the bidding strategy set $\Omega_{\tilde{\mathbf{e}}_n}$ in (2), and the sets $\Omega_{\mathbf{g}_n}$ and $\Omega_{\mathbf{s}_n}$ introduced in Section II-B, the overall strategy set for a generic user $n \in \mathcal{N}$ is given by

$$\Omega_{\mathbf{x}_n} \triangleq \big\{\mathbf{x}_n \in \mathbb{R}^{3H} : \tilde{\mathbf{e}}_n \in \Omega_{\tilde{\mathbf{e}}_n}, \mathbf{g}_n \in \Omega_{\mathbf{g}_n}, \mathbf{s}_n \in \Omega_{\mathbf{s}_n}\big\} \tag{5}$$

with $\mathbf{g}_n = \mathbf{0}$ if $n \notin \mathcal{G}$ and $\mathbf{s}_n = \mathbf{0}$ if $n \notin \mathcal{S}$.

B. Energy Cost and Pricing Model

This section introduces the cost model regulating the energy prices. Typically, during the day-ahead market, the different energy generators in the supply-side (each of them characterized by a specific price curve) submit their production offers; likewise, consumers and retailers submit their consumption bids. This process determines the energy prices and the traded quantities [2, Ch. 1.2]. Since in the present paper we are

[3] Non-dispatchable sources, having only fixed costs, imply no strategy regarding energy production, unlike dispatchable generators (see Section II-B).

[4] Energy storage bears implicit costs related to the intrinsic inefficiency of the storage device, e.g., eventual leakage (see Section VI) or non-ideal charging/discharging efficiencies (cf. [14]), rather than direct variable costs as dispatchable generation.

This article has been accepted for publication in a future issue of this journal, but has not been fully edited. Content may change prior to final publication. Citation information: DOI 10.1109/TSP.2014.2307835, IEEE Transactions on Signal Processing

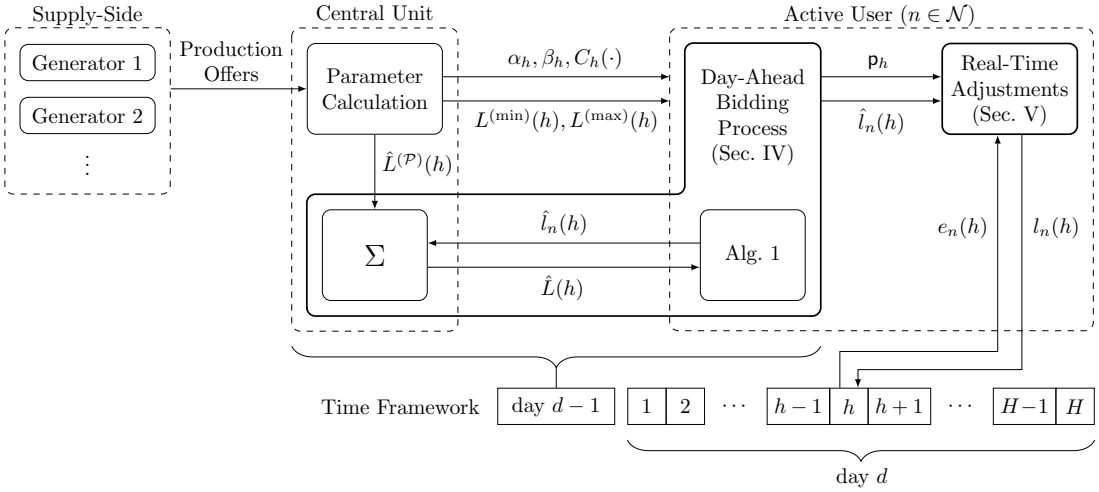

Fig. 2. Schematic representation of the proposed DSM method, consisting of day-ahead bidding process and real-time adjustments.

particularly interested in the demand-side of the network, we can abstract this procedure by considering a single price curve resulting from aggregating the individual curves of each generator in the supply-side; this is a well-established procedure in the smart grid literature (c.f. [7], [10], [21]).

With this objective in mind, let $C_h(\cdot)$ be the function indicating the *cost per unit of energy* at time-slot h. Within the day-ahead bidding process, demand-side users induce the *per-slot aggregate bid energy load* $\tilde{L}(h)$ and thus determine the price per unit of energy $C_h\big(\tilde{L}(h)\big)$, which remains fixed during the day period. In this paper, we adopt a linear cost function per unit of energy:

$$C_h\big(\tilde{L}(h)\big) = K_h \tilde{L}(h). \tag{6}$$

The overall variable costs to supply the amount $\tilde{L}(h)$ are then given by $C_h\big(\tilde{L}(h)\big)\tilde{L}(h) = K_h \tilde{L}^2(h)$, which corresponds to the quadratic grid cost function widely used in the smart grid literature (e.g., in [7], [10]). In general, the grid coefficients $K_h > 0$ are different at each time-slot h, since the energy production varies along the day period according to the aggregate energy demand and to the availability of intermittent energy sources.

Let $\hat{L}^{(\mathcal{P})}(h)$ denote the predicted per-slot aggregate energy consumption associated with the passive users: then, the per-slot aggregate bid energy load $\tilde{L}(h)$ can be expressed as

$$\tilde{L}(h) \triangleq \hat{L}^{(\mathcal{P})}(h) + \sum_{n \in \mathcal{N}} \tilde{l}_n(h) \tag{7}$$

which depends on the users' strategies through $\tilde{l}_n(h)$ in (3), and is subject to the following global constraint.

Constraint 1 (on the per-slot aggregate bid energy load). The per-slot aggregate bid energy load in (7) must satisfy

$$L^{(\min)}(h) \le \tilde{L}(h) \le L^{(\max)}(h), \qquad \forall h \tag{8}$$

where $L^{(\min)}(h) > 0$ (resp. $L^{(\max)}(h) > 0$) denotes the minimum (resp. the maximum) per-slot aggregate energy load within which $C_h\big(\tilde{L}(h)\big)$ resembles the energy price curve obtained by aggregating the production costs of the individual energy generators in the supply-side. In particular, a real-time aggregate demand lower than $L^{(\min)}(h)$ may imply additional costs for the supply-side if this requires turning off some base load power plant [16]. On the other hand, $L^{(\max)}(h)$ can be interpreted as the upper bound on the per-slot aggregate bid energy load that allows to satisfy the real-time aggregate demand with a certain outage probability. Alternatively, these boundaries can be chosen to guarantee a certain PAR of the real-time aggregate load with high probability. We suppose that the central unit can set $L^{(\min)}(h)$, $L^{(\max)}(h)$ and predict $\hat{L}^{(\mathcal{P})}(h)$ based on the available past statistics; an overview on load forecasting techniques can be found in [24].

Each active user $n \in \mathcal{N}$ derives his *bid energy load vector* $\tilde{\mathbf{l}}_n \triangleq \big(\tilde{l}_n(h)\big)_{h=1}^{H}$ during the day-ahead demand-side bidding process. At a given time-slot h, if the user attains to his day-ahead bid $\tilde{l}_n(h)$, he simply pays $K_h \tilde{L}(h)\tilde{l}_n(h)$; otherwise, he can possibly deviate from $\tilde{l}_n(h)$ by purchasing/selling a different amount of energy $l_n(h)$, for which he pays/perceives $K_h \tilde{L}(h) l_n(h)$, while incurring in the following penalties:

$$\alpha_h K_h \tilde{L}(h)\big(l_n(h) - \tilde{l}_n(h)\big), \qquad \text{if } l_n(h) > \tilde{l}_n(h) \tag{9}$$

$$\beta_h K_h \tilde{L}(h)\big(\tilde{l}_n(h) - l_n(h)\big), \qquad \text{if } l_n(h) < \tilde{l}_n(h) \tag{10}$$

where $\alpha_h, \beta_h \in (0, 1]$ are the penalty parameters for exceeding and for falling behind the negotiated load $\tilde{l}_n(h)$, respectively.

Given the bid energy loads $\big\{\tilde{l}_n(h)\big\}_{h=1}^{H}$, the *cumulative monetary expense* incurred by user $n \in \mathcal{N}$ for exchanging the energy loads $\big\{l_n(h)\big\}_{h=1}^{H}$ with the grid (including the aforementioned penalties for deviations and taking into account the amount of produced energy $\big\{g_n(h)\big\}_{h=1}^{H}$) can be expressed as[5]

$$\mathsf{p}_n^{(\mathcal{N})}(\tilde{\mathbf{l}}_n, \tilde{\mathbf{l}}_{-n}) \triangleq \sum_{h=1}^{H} K_h\big(\tilde{L}_{-n}(h) + \tilde{l}_n(h)\big) \times \Big(l_n(h) + \vartheta_h\big(l_n(h) - \tilde{l}_n(h)\big)\Big) + \sum_{h=1}^{H} W_n\big(g_n(h)\big) \tag{11}$$

[5]In light of the described penalty system, $L^{(\min)}(h)$ in (8) also prevents the active users from intentionally decreasing the aggregate bid energy load $\tilde{L}(h)$ to the level below which the penalties given by α_h are insufficient to compensate for the additional generation costs of the upward real-time deviations.

This article has been accepted for publication in a future issue of this journal, but has not been fully edited. Content may change prior to final publication. Citation information: DOI 10.1109/TSP.2014.2307835, IEEE Transactions on Signal Processing

where $\tilde{\mathbf{l}}_{-n} \triangleq \big(\tilde{l}_{-n}(h)\big)_{h=1}^{H}$ is the aggregate bid energy load vector of the other users, with

$$\tilde{l}_{-n}(h) \triangleq \tilde{L}(h) - \tilde{l}_n(h) = \hat{L}^{(\mathcal{P})}(h) + \sum_{m \in \mathcal{N}\setminus\{n\}} \tilde{l}_m(h) \quad (12)$$

and where we have introduced the penalty function

$$\vartheta_h(x) \triangleq \alpha_h (x)^+ + \beta_h (-x)^+. \quad (13)$$

The penalty parameters $\big\{\alpha_h, \beta_h\big\}_{h=1}^{H}$ are established before the day-ahead bidding process with the objective of discouraging real-time deviations from the bid loads, either upwards or downwards. For instance, the central unit would choose $\alpha_h > \beta_h$ during hours of high expected consumption, and $\alpha_h < \beta_h$ during hours of low expected consumption.

The proposed pricing model does not explicitly deal with the billing of passive users, as our DSM method is not thereby affected. However, in order to encourage demand-side participation in the bidding process, passive users may be penalized with respect to the active ones by applying an overprice to the purchased energy; see Appendix I-A for more details.

C. Proposed DSM Approach

In our DSM procedure, the active users individually optimize their bidding, production, and storage strategies at two different time granularities, i.e., day-ahead and real-time, as illustrated in Fig. 2. Before going into the detailed description, let us summarize the temporal sequence of the proposed DSM method.

Day-ahead optimization (c.f. Section IV). In the day-ahead bidding process, the users' goal is to minimize their individual expected cumulative expense over the day period

$$\mathsf{f}_n(\mathbf{x}_n, \tilde{\mathbf{l}}_{-n}) \triangleq \mathsf{E}\big\{\mathsf{p}_n^{(\mathcal{N})}(\boldsymbol{\Delta}\mathbf{x}_n, \tilde{\mathbf{l}}_{-n})\big\} \quad (14)$$

where $\boldsymbol{\Delta} \triangleq (\mathbf{I}_H \otimes \boldsymbol{\delta})^{\mathrm{T}}$ and $\boldsymbol{\delta} \triangleq (1, -1, 1)$, so that $\boldsymbol{\delta}^{\mathrm{T}}\mathbf{x}_n(h) = \tilde{l}_n(h)$ and $\boldsymbol{\Delta}\mathbf{x}_n = \tilde{\mathbf{l}}_n$. The expected cumulative expense in (14) is obtained in closed-form as given in Lemma 1, where we have introduced the following notation:

$$\phi_{e_n(h)}\big(\mathbf{x}_n(h)\big) \triangleq \mathsf{E}\big\{l_n(h) + \vartheta_h\big(l_n(h) - \boldsymbol{\delta}^{\mathrm{T}}\mathbf{x}_n(h)\big)\big\} \quad (15)$$

$$= (1+\alpha_h)\bar{e}_n(h) - g_n(h) + s_n(h) - \alpha_h \tilde{e}_n(h)$$
$$+ (\alpha_h + \beta_h)\big(\tilde{e}_n(h) F_{e_n(h)}\big(\tilde{e}_n(h)\big) - G_{e_n(h)}\big(\tilde{e}_n(h)\big)\big) \quad (16)$$

$$G_{e_n(h)}(x) \triangleq \int_{-\infty}^{x} t f_{e_n(h)}(t) dt \quad (17)$$

$\bar{e}_n(h) \triangleq \mathsf{E}\{e_n(h)\}$, and $\boldsymbol{\delta}_g \triangleq (0, 1, 0)$.

Lemma 1 (Expected Cumulative Expense). Given the per-slot bid energy loads $\tilde{\mathbf{l}}_n$, the expected cumulative expense $\mathsf{f}_n(\mathbf{x}_n, \tilde{\mathbf{l}}_{-n})$ in (14) is given by

$$\mathsf{f}_n(\mathbf{x}_n, \tilde{\mathbf{l}}_{-n}) = \sum_{h=1}^{H} K_h\big(\tilde{l}_{-n}(h) + \boldsymbol{\delta}^{\mathrm{T}}\mathbf{x}_n(h)\big)\phi_{e_n(h)}\big(\mathbf{x}_n(h)\big) + \sum_{h=1}^{H} W_n\big(\boldsymbol{\delta}_g^{\mathrm{T}}\mathbf{x}_n(h)\big). \quad (18)$$

Proof. See Appendix I-B.

The grid coefficients $\big\{K_h\big\}_{h=1}^{H}$ and the penalty parameters $\big\{\alpha_h, \beta_h\big\}_{h=1}^{H}$ are fixed before the day-ahead bidding process [8], [22] and broadcast to the demand-side users. Then, each active user reacts to the prices $\big\{K_h \tilde{L}(h)\big\}_{h=1}^{H}$ provided by the central unit through iteratively adjusting his per-slot bid energy load vector $\tilde{\mathbf{l}}_n$. Here, his goal is to minimize his expected cumulative expense, subject to both local and global requirements given by $\Omega_{\mathbf{x}_n}$ and Constraint 1, respectively. This optimization problem, however, is not convex and calls for a centralized optimization, which would lead to non-scalable solution algorithms and privacy issues (see [15] for details). For this reason, in this paper we focus on more appealing distributed system designs, as described in Section IV.

Real-time optimization (c.f. Section V). Once the day-ahead bidding process finalizes, the prices per unit of energy $\big\{K_h \tilde{L}(h)\big\}_{h=1}^{H}$ remain fixed. However, as the dispatch time-slot approaches, active users have more reliable information about their energy needs. Hence, they can exploit this coming information to adjust their production and storage strategies $\mathbf{g}_n$ and $\mathbf{s}_n$ in real-time. In doing so, they aim at reducing the deviation of the real-time strategy with respect to the bid energy load, i.e., $\big|l_n(h) - \tilde{l}_n(h)\big|$, so as to minimize their expected expense for the rest of the day period.

After performing the day-ahead and the real-time optimization, the active users are finally billed according to (11).

IV. Day-Ahead DSM for Expected Cost Minimization

In this section, we formulate the day-ahead bidding system introduced in Section III as a generalized Nash equilibria problem (GNEP). To this end, we first introduce some preliminary definitions. Let us rewrite Constraint 1 in the form of shared constraints $\mathbf{q}(\mathbf{x}) \leq \mathbf{0}$, where $\mathbf{q}(\mathbf{x}) \triangleq (\mathbf{q}^{(\min)}(\mathbf{x}), \mathbf{q}^{(\max)}(\mathbf{x})) : \mathbb{R}^{3HN} \to \mathbb{R}^{2H}$ with $\mathbf{x} \triangleq \big(\mathbf{x}_n\big)_{n=1}^{N}$ and

$$\mathbf{q}^{(\min)}(\mathbf{x}) \triangleq \Big(L^{(\min)}(h) - \sum_{n \in \mathcal{N}} \boldsymbol{\delta}^{\mathrm{T}}\mathbf{x}_n(h) - \hat{L}^{(\mathcal{P})}(h)\Big)_{h=1}^{H} \quad (19)$$

$$\mathbf{q}^{(\max)}(\mathbf{x}) \triangleq \Big(\sum_{n \in \mathcal{N}} \boldsymbol{\delta}^{\mathrm{T}}\mathbf{x}_n(h) + \hat{L}^{(\mathcal{P})}(h) - L^{(\max)}(h)\Big)_{h=1}^{H}.$$

Note that $\mathbf{q}(\mathbf{x})$ is convex in $\mathbf{x} \in \Omega_{\mathbf{x}} \triangleq \prod_{n \in \mathcal{N}} \Omega_{\mathbf{x}_n}$. The strategy set of user $n \in \mathcal{N}$ can be then expressed as (c.f. (5))

$$\Theta_{\mathbf{x}_n}(\tilde{\mathbf{l}}_{-n}) \triangleq \big\{\mathbf{x}_n \in \Omega_{\mathbf{x}_n} : \mathbf{q}(\mathbf{x}_n, \tilde{\mathbf{l}}_{-n}) \leq \mathbf{0}\big\} \quad (20)$$

whereas the joint strategy set is given by

$$\Theta_{\mathbf{x}} \triangleq \big\{\mathbf{x} \in \mathbb{R}^{3HN} : \mathbf{x}_n \in \Omega_{\mathbf{x}_n}, \forall n \in \mathcal{N} \text{ and } \mathbf{q}(\mathbf{x}) \leq \mathbf{0}\big\}. \quad (21)$$

We formulate the system design as the GNEP $\mathscr{G} = \big\langle \Theta_{\mathbf{x}}, \mathbf{f} \big\rangle$, with $\Theta_{\mathbf{x}}$ given in (21), $\mathbf{f} \triangleq \big(\mathsf{f}_n(\mathbf{x}_n, \tilde{\mathbf{l}}_{-n})\big)_{n=1}^{N}$, and $\mathsf{f}_n(\mathbf{x}_n, \tilde{\mathbf{l}}_{-n})$ defined in (18). Here, each user is a player who aims at minimizing his expected cumulative expense subject to both individual and global constraints (c.f. (20)):

$$\begin{aligned} \min_{\mathbf{x}_n} \quad & \mathsf{f}_n(\mathbf{x}_n, \tilde{\mathbf{l}}_{-n}) \\ \text{s.t.} \quad & \mathbf{x}_n \in \Theta_{\mathbf{x}_n}(\tilde{\mathbf{l}}_{-n}) \end{aligned} \qquad \forall n \in \mathcal{N}. \quad (22)$$

This article has been accepted for publication in a future issue of this journal, but has not been fully edited. Content may change prior to final publication. Citation information: DOI 10.1109/TSP.2014.2307835, IEEE Transactions on Signal Processing

The GNEP $\mathscr{G} = \left\langle \Theta_{\mathbf{x}}, \mathbf{f} \right\rangle$ is the problem of finding a feasible strategy profile $\mathbf{x}^\star \triangleq \left(\mathbf{x}_n^\star\right)_{n=1}^N$ such that $\mathsf{f}_n(\mathbf{x}_n^\star, \tilde{\mathbf{l}}_{-n}^\star) \leq \mathsf{f}_n(\mathbf{x}_n, \tilde{\mathbf{l}}_{-n}^\star), \forall \mathbf{x}_n \in \Theta_{\mathbf{x}_n}(\tilde{\mathbf{l}}_{-n}^\star)$, for all players $n \in \mathcal{N}$ [25]. The solution of the GNEP is called (generalized) Nash equilibrium. We refer to [17, Sec. 4.3] for a detailed overview on GNEPs.

A. Variational Solutions

GNEPs with shared constraints such as (22) are difficult problems to solve. They can be formulated as quasi-variational inequality (QVI) problems [19]; however, in spite of some interesting and promising recent advancements (see, e.g., [26], [27]), no efficient numerical methods based on the QVI reformulation have been developed yet. Nevertheless, for this type of GNEPs, some VI techniques can still be employed [17].

Definition 1 ([19, Def. 1.1.1])**.** *Given the vector-valued function $\mathbf{F} : \Theta_{\mathbf{x}} \to \mathbb{R}^{3HN}$ with $\Theta_{\mathbf{x}}$ defined in* (21)*, the VI problem* $\mathrm{VI}(\Theta_{\mathbf{x}}, \mathbf{F})$ *consists in finding a point $\mathbf{x}^\star \in \Theta_{\mathbf{x}}$ such that*

$$(\mathbf{x} - \mathbf{x}^\star)^{\mathrm{T}} \mathbf{F}(\mathbf{x}^\star) \geq 0, \qquad \forall \mathbf{x} \in \Theta_{\mathbf{x}}. \tag{23}$$

Indeed a solution of the GNEP can be computed by solving a suitably defined VI problem, as stated in the next lemma, whose proof is based on standard techniques [17], [28], [29]; see Appendix II-A for more details.

Lemma 2. Given the GNEP $\mathscr{G} = \left\langle \Theta_{\mathbf{x}}, \mathbf{f} \right\rangle$, suppose that the following conditions are satisfied: for all $n \in \mathcal{N}$,

(a) The strategy sets $\Omega_{\mathbf{g}_n}$ and $\Omega_{\mathbf{s}_n}$ are closed and convex;
(b) The production cost function $W_n(x)$ is convex, $\forall n \in \mathcal{G}$;
(c) $\chi_n^{(\min)}(h)$ and $\chi_n^{(\max)}(h)$ in (2) are chosen such that the pdf of the per-slot net energy consumption satisfies

$$f_{e_n(h)}(x) \geq \frac{1}{(\alpha_h + \beta_h) L^{(\min)}(h)} \frac{\left(\alpha_h + 1\right)^2}{2} \tag{24}$$

$\forall x \in \left[\chi_n^{(\min)}(h), \chi_n^{(\max)}(h)\right]$.

Let $\mathbf{F}(\mathbf{x}) \triangleq \left(\nabla_{\mathbf{x}_n} \mathsf{f}_n(\mathbf{x}_n, \tilde{\mathbf{l}}_{-n})\right)_{n=1}^N$. Then, every solution of the $\mathrm{VI}(\Theta_{\mathbf{x}}, \mathbf{F})$ is a solution of the GNEP.

Remark 1 (on Lemma 2). (a) Given $\Omega_{\tilde{\mathbf{e}}_n}$ in (2), the closeness and convexity of $\Omega_{\mathbf{g}_n}$ and $\Omega_{\mathbf{s}_n}$ ensure the same properties for the strategy set $\Omega_{\mathbf{x}_n}$ in (5). For instance, the dispatchable production and storage models adopted in [14] and evoked in Section VI enjoy such properties. (b) The convexity of $W_n(\cdot)$ simply implies that the production cost function does not tend to saturate as $g_n(h)$ increases [14, Remark 1.1]. (c) When the distribution of $e_n(h)$ is unimodal, condition (24) limits the displacement of $\tilde{e}_n(h)$ around the mode of $e_n(h)$ in order to ensure the convexity of the objective function $\mathsf{f}_n(\mathbf{x}_n, \tilde{\mathbf{l}}_{-n})$. On the contrary, when the distribution of $e_n(h)$ is multimodal, $\chi_n^{(\min)}(h)$ and $\chi_n^{(\max)}(h)$ must be carefully selected to guarantee the convexity of $\mathsf{f}_n(\mathbf{x}_n, \tilde{\mathbf{l}}_{-n})$. A heuristic procedure to deal with such cases is presented in Appendix II-B. These considerations also apply to condition (27) given in Theorem 1(a.2).

Note that, when passing from the GNEP (22) to the associated VI, not all the GNEP's solutions are preserved: Lemma 2 in fact does not state that any solution of the GNEP is also a solution of the VI (see [30] for further details and examples). The solutions of the GNEP that are also solutions of the $\mathrm{VI}(\Theta_{\mathbf{x}}, \mathbf{F})$ are termed as *variational solutions* [17], [30] and enjoy some remarkable properties that make them particularly appealing in many applications. Among all, they can be interpreted as the solutions of a Nash equilibrium problem (NEP) with pricing, as detailed next.

Consider the following augmented NEP with $N+1$ players, in which the "new" $(N+1)$-th player (at the same level of the other N players) controls the price variable $\boldsymbol{\lambda} \in \mathbb{R}_+^{2H}$:

$$\begin{array}{ll} \min\limits_{\mathbf{x}_n} & \mathsf{f}_n(\mathbf{x}_n, \tilde{\mathbf{l}}_{-n}) + \boldsymbol{\lambda}^{\mathrm{T}} \mathbf{q}(\mathbf{x}_n, \tilde{\mathbf{l}}_{-n}) \\ \text{s.t.} & \mathbf{x}_n \in \Omega_{\mathbf{x}_n} \end{array} \qquad \forall n \in \mathcal{N} \tag{25}$$

$$\min_{\boldsymbol{\lambda} \geq \mathbf{0}} \quad -\boldsymbol{\lambda}^{\mathrm{T}} \mathbf{q}(\mathbf{x}).$$

We can interpret $\boldsymbol{\lambda}$ as the overprices applied to force the users to satisfy the shared constraints $\mathbf{q}(\mathbf{x})$. Indeed, when $\mathbf{q}(\mathbf{x}) \leq \mathbf{0}$, the optimal price will be $\boldsymbol{\lambda} = \mathbf{0}$ (there is no need to punish the users if the constraints are already satisfied).

We can now establish the connection between the $\mathrm{VI}(\Theta_{\mathbf{x}}, \mathbf{F})$ and the augmented NEP (25) [17, Lem. 4.4].

Lemma 3. Under the setting of Lemma 2, $(\mathbf{x}^\star, \boldsymbol{\lambda}^\star)$ is a Nash equilibrium of the NEP (25) if and only if $\mathbf{x}^\star$ is a solution of the $\mathrm{VI}(\Theta_{\mathbf{x}}, \mathbf{F})$, i.e., a variational solution of the GNEP $\mathscr{G} = \left\langle \Theta_{\mathbf{x}}, \mathbf{f} \right\rangle$, and $\boldsymbol{\lambda}^\star$ is the multiplier associated with the shared constraints $\mathbf{q}(\mathbf{x}^\star) \leq \mathbf{0}$ in $\Theta_{\mathbf{x}}$.

Based on Lemma 3, we are now able to analyze and compute the variational solutions of the GNEP (22) as solutions of the NEP (25), building on recent results in [31]. The following is a standard existence result of variational solutions, based on solution analysis of VIs [19].

Lemma 4. Given the GNEP $\mathscr{G} = \left\langle \Theta_{\mathbf{x}}, \mathbf{f} \right\rangle$, suppose that: i) conditions in Lemma 2 are satisfied; and ii) the strategy sets $\Omega_{\mathbf{g}_n}$ and $\Omega_{\mathbf{s}_n}$ are bounded. Then, the GNEP has variational solutions.

In the next section, we build on the game theoretical pricing-based interpretation (25) (c.f. Lemma 3) to design distributed algorithms that converge to a variational solution of the GNEP.

B. Distributed Algorithms

We focus on the class of *totally asynchronous* best-response algorithms, where some users may update their strategies more frequently than others and they may even use outdated information about the strategy profiles adopted by the other users. Let $\mathscr{T}_n \subseteq \mathscr{T} \subseteq \{0, 1, 2, \ldots\}$ be the set of times at which user $n \in \mathcal{N}$ updates his own strategy $\mathbf{x}_n$, denoted by $\mathbf{x}_n^{(i)}$ at the ith iteration. We use $t_n(i)$ to denote the most recent time at which the strategy of user n is perceived by the central unit at the ith iteration. We assume that some standard conditions in asynchronous convergence theory (see (A1)–(A3) in [15, Sec III-C]), which are fulfilled in any practical implementation, hold for $\mathscr{T}_n$ and $t_n(i)$, $\forall n \in \mathcal{N}$.

According to the asynchronous scheduling, each user updates his strategy by minimizing his cumulative expense over the day period, given the most recently available value of the per-slot aggregate bid energy load

This article has been accepted for publication in a future issue of this journal, but has not been fully edited. Content may change prior to final publication. Citation information: DOI 10.1109/TSP.2014.2307835, IEEE Transactions on Signal Processing

$$\tilde{L}^{(\mathbf{t}(i))}(h) \triangleq \hat{L}^{(\mathcal{P})}(h) + \sum_{m\in\mathcal{N}} \tilde{l}_m^{(t_m(i))}(h) \tag{26}$$

that considers the bid energy loads of the other users as perceived by the central unit, which can possibly be outdated when computation occurs. Each user n then obtains $\tilde{\mathbf{l}}_{-n}^{(\mathbf{t}(i))} \triangleq \big(\tilde{l}_{-n}^{(\mathbf{t}(i))}(h)\big)_{h=1}^{H}$, with $\tilde{l}_{-n}^{(\mathbf{t}(i))}(h) \triangleq \tilde{L}^{(\mathbf{t}(i))}(h) - \tilde{l}_n^{(t_n(i))}(h)$.

We can compute the variational solutions of the GNEP (22) by solving the augmented NEP (25). This can be done using the recent framework in [31], which leads to the asynchronous proximal decomposition algorithm (PDA) described in Algorithm 1, and whose convergence conditions are given in Theorem 1.

Algorithm 1 Asynchronous PDA with Coupling Constraints

`Data` : Set $i=0$ and the initial centroids $\big(\bar{\mathbf{x}}_n\big)_{n=1}^{N} = \mathbf{0}$ and $\bar{\boldsymbol{\lambda}} = \mathbf{0}$. Given $\big\{K_h, \alpha_h, \beta_h\big\}_{h=1}^{H}$, $\big\{\rho^{(i)}\big\}_{i=0}^{\infty}$, $\tau > 0$, and any feasible starting point $\mathbf{z}^{(0)} \triangleq \big(\big(\mathbf{x}_n^{(0)}\big)_{n=1}^{N}, \boldsymbol{\lambda}^{(0)}\big)$ with $\boldsymbol{\lambda}^{(0)} \geq \mathbf{0}$:

`(S.1)` : `If` a suitable termination criterion is satisfied: `STOP`.

`(S.2)` : `For` $n \in \mathcal{N}$, each user computes $\mathbf{x}_n^{(i+1)}$ as

$$\mathbf{x}_n^{(i+1)} = \begin{cases} \mathbf{x}_n^{\star} \in \underset{\mathbf{x}_n\in\Omega_{\mathbf{x}_n}}{\operatorname{argmin}} \Big\{ \mathsf{f}_n\big(\mathbf{x}_n, \tilde{\mathbf{l}}_{-n}^{(\mathbf{t}(i))}\big) \\ \qquad +(\boldsymbol{\lambda}^{(i)})^{\mathrm{T}}\mathbf{q}\big(\mathbf{x}_n, \tilde{\mathbf{l}}_{-n}^{(\mathbf{t}(i))}\big) + \frac{\tau}{2}\|\mathbf{x}_n - \bar{\mathbf{x}}_n\|^2 \Big\}, \\ \qquad\qquad\qquad\qquad\qquad \text{if } i \in \mathcal{T}_n \\ \mathbf{x}_n^{(i)}, \qquad\qquad\qquad\qquad\qquad \text{otherwise} \end{cases}$$

`End`

The central unit computes $\boldsymbol{\lambda}^{(i+1)}$ as

$$\boldsymbol{\lambda}^{(i+1)} = \boldsymbol{\lambda}^{\star} \in \underset{\boldsymbol{\lambda}\geq\mathbf{0}}{\operatorname{argmin}} \Big\{ -\boldsymbol{\lambda}^{\mathrm{T}}\mathbf{q}(\mathbf{x}) + \frac{\tau}{2}\|\boldsymbol{\lambda} - \bar{\boldsymbol{\lambda}}\|^2 \Big\}$$

`(S.3)` : `If` the NE is reached, then each user $n \in \mathcal{N}$ sets $\mathbf{x}_n^{(i+1)} \leftarrow (1-\rho^{(i)})\bar{\mathbf{x}}_n + \rho^{(i)}\mathbf{x}_n^{(i+1)}$ and updates his centroid: $\bar{\mathbf{x}}_n = \mathbf{x}_n^{(i+1)}$; likewise, the central unit sets $\boldsymbol{\lambda}^{(i+1)} \leftarrow (1-\rho^{(i)})\bar{\boldsymbol{\lambda}} + \rho^{(i)}\boldsymbol{\lambda}^{(i+1)}$ and updates the centroid: $\bar{\boldsymbol{\lambda}} = \boldsymbol{\lambda}^{(i+1)}$.

`(S.4)` : $i \leftarrow i+1$; `Go to (S.1).`

Theorem 1. *Given the GNEP $\mathscr{G} = \langle \Theta_{\mathbf{x}}, \mathbf{f}\rangle$, suppose that:*

(a.1) *Conditions* (a)–(b) *in Lemma* 2 *are satisfied;*

(a.2) $\chi_n^{(\min)}(h)$ *and* $\chi_n^{(\max)}(h)$ *in* (2) *are chosen such that the pdf of the per-slot net energy consumption satisfies*

$$f_{e_n(h)}(x) \geq \frac{1}{(\alpha_h+\beta_h)L^{(\min)}(h)}\Big(\frac{(\alpha_h+1)^2}{4} + N\big(\max(\alpha_h,\beta_h) + \alpha_h + \beta_h\big)\Big) \tag{27}$$

$\forall x \in \big[\chi_n^{(\min)}(h), \chi_n^{(\max)}(h)\big]$, *for all* $n \in \mathcal{N}$;

(a.3) *The penalty parameters are such that* $\alpha_h + \beta_h \leq 1, \forall h$;

(b) *The regularization parameter* τ *satisfies*

$$\tau > \frac{3}{2}(N-1)\max_h K_h + \sqrt{\frac{9}{4}(N-1)^2 \max_h K_h^2 + 3HN} \tag{28}$$

(c) $\{\rho^{(i)}\} \subset [R_m, R_M]$, *with* $0 < R_m < R_M < 2$.

Then, any sequence $\big\{(\mathbf{x}^{(i)}, \boldsymbol{\lambda}^{(i)})\big\}_{i=1}^{\infty}$ *generated by Algorithm* 1 *converges to a variational solution of the GNEP.*

Proof. See Appendix II-C.

Remark 2 (**on Algorithm 1**)**.** Algorithm 1 is a double-loop algorithm in nature. The inner loop requires the solution of the regularized game in `(S.3)` via asynchronous best-response algorithms. In the outer loop, all users $n \in \mathcal{N}$ and the central unit, which acts as the $(N+1)$-th player, update the centroids $\{\bar{\mathbf{x}}_n\}_{n\in\mathcal{N}}, \bar{\boldsymbol{\lambda}}$ and proceed to solve the inner game again, until an equilibrium is reached. Observe that the update of $\{\bar{\mathbf{x}}_n\}_{n\in\mathcal{N}}$ is performed locally by the users at the cost of no signaling exchange with the central unit.

Remark 3 (**on Theorem 1**)**.** The regularization parameter τ determines the trade-off between the convergence stability and the convergence speed [31]. The peculiarity of the expression of τ provided in (28) is that it can be calculated by the central unit a priori without interfering with the privacy of the users.

At the beginning of the optimization process, τ is computed as in (28) and broadcast, together with the grid coefficients and the penalty parameters $\big\{K_h, \alpha_h, \beta_h\big\}_{h=1}^{H}$, to the demand-side. At each iteration, any active user can update his strategy by minimizing his objective function (18) based on the most recent values of the aggregate bid energy loads $\big\{\tilde{L}^{(\mathbf{t}(i))}(h)\big\}_{h=1}^{H}$, which are calculated by the central unit referring to the (possibly outdated) individual demands. At the same time, the central unit updates the price variable $\boldsymbol{\lambda}$ and broadcasts it to the demand-side. When the equilibrium in `(S.3)` is reached, the central unit initiates a new iteration. Observe that it is not necessary to compute the Nash equilibrium in the inner loop exactly; indeed, inexact solutions do not affect the convergence of Algorithm 1 as long as the error bound goes to zero as the number of iterations grows [17], [20]. This process is repeated until some convergence criterion established by the central unit is fulfilled.

Note that, if we omit Constraint 1 (cf. (8)), the GNEP (22) reduces to a classical NEP, where the coupling among the players occurs only at the level of the objective functions (as addressed in [32]). Of course, the framework and algorithm proposed in the present paper contain this formulation as special case.

V. Real-Time Adjustments of the Production and Storage Strategies

In real-time, active users reasonably know the values of their net energy consumption $e_n(h)$ for the upcoming time-slot with much less uncertainty than during the day-ahead bidding process. In this section, we describe how the users can profit from this fact and perform real-time adjustments to the calculated production and storage strategies in order to reduce the impact of the day-ahead uncertainty.

After the day-ahead bidding process, the prices per unit of energy $\big\{\mathsf{p}_h = K_h\tilde{L}(h)\big\}_{h=1}^{H}$ are fixed as a result of the energy bid loads of the active users obtained with Algorithm 1. Then, active users are charged in real-time based on such prices, while the differences between their actual energy requirements

This article has been accepted for publication in a future issue of this journal, but has not been fully edited. Content may change prior to final publication. Citation information: DOI 10.1109/TSP.2014.2307835, IEEE Transactions on Signal Processing

and the negotiated day-ahead amounts are subject to the penalties described in Section III-B (c.f. (11)). In this setting, at each h, active user $n \in \mathcal{N}$ can exploit the reduced uncertainty about his net energy consumption $e_n(h)$ to independently adjust his production and storage strategies $\{g_n(t), s_n(t)\}_{t=h}^{H}$ so as to minimize his expected expense for the remaining time-slots $t = h, \ldots, H$. At the same time, we can guarantee the following individual constraints on the per-slot energy load.

Constraint 2 (on the per-slot energy load). Due to physical constraints on the user's individual distribution infrastructure, the per-slot energy load $l_n(h)$ in (1) is bounded as

$$-l_n^{(\min)} \leq l_n(h) \leq l_n^{(\max)}, \qquad \forall h \tag{29}$$

where $l_n^{(\min)} \geq 0$ and $l_n^{(\max)} > 0$ are the outgoing and the incoming capacities of user n's energy link, respectively.

For modeling simplicity, we assume that, right before each time-slot h, each user $n \in \mathcal{N}$ has perfect knowledge of $e_n(h)$. Nonetheless, he still needs to satisfy the requirements given by his production and storage strategy sets $\Omega_{\mathbf{g}_n}$ and $\Omega_{\mathbf{s}_n}$: in this regard, if the strategies over different time-slots are coupled (see, e.g., the constraints in Table I), the users have to take into account the strategies adopted in the previous time-slots. With this objective in mind, let $\mathbf{y}_n(h) \triangleq \big(g_n(h), s_n(h)\big)$ denote the real-time strategy for each time-slot h, and let $\big(g_n^\star(t)\big)_{t=1}^{h-1}$ and $\big(s_n^\star(t)\big)_{t=1}^{h-1}$ express the production and storage strategies already fixed in the past time-slots $t = 1, \ldots, h-1$. Then, the real-time strategy set for user $n \in \mathcal{N}$ at h is defined as in (30) at the bottom of the page.

Hence, the price paid by user $n \in \mathcal{N}$ for purchasing energy from the grid at time-slot h (conditioned on the bid load $\tilde{l}_n(h)$) is given by

$$\begin{aligned}\mathsf{p}_{n,h}^{(\mathcal{N})}\big(\mathbf{y}_n(h) \mid \tilde{l}_n(h)\big) &\triangleq \mathsf{p}_h\big(e_n(h) + \boldsymbol{\delta}_{s-g}^{\mathrm{T}}\mathbf{y}_n(h) \\ &+ \vartheta_h\big(e_n(h) + \boldsymbol{\delta}_{s-g}^{\mathrm{T}}\mathbf{y}_n(h) - \tilde{l}_n(h)\big)\big) + W_n\big(\boldsymbol{\delta}_g^{\mathrm{T}}\mathbf{y}_n(h)\big)\end{aligned} \tag{31}$$

where $\vartheta_h(x)$ is defined in (13), $\boldsymbol{\delta}_{s-g} \triangleq (-1, 1)$, and where we have conveniently redefined $\boldsymbol{\delta}_g \triangleq (1, 0)$. Likewise, the expected expense for each time-slot $t = h+1, \ldots, H$ is

$$\begin{aligned}\mathsf{f}_{n,t}\big(\mathbf{y}_n(t) \mid \tilde{l}_n(t)\big) &\triangleq \mathsf{p}_t\mathsf{E}\big\{e_n(t) + \boldsymbol{\delta}_{s-g}^{\mathrm{T}}\mathbf{y}_n(t) \\ &+ \vartheta_t\big(e_n(t) + \boldsymbol{\delta}_{s-g}^{\mathrm{T}}\mathbf{y}_n(t) - \tilde{l}_n(t)\big)\big\} + W_n\big(\boldsymbol{\delta}_g^{\mathrm{T}}\mathbf{y}_n(t)\big)\end{aligned} \tag{32}$$

which can be easily calculated in closed-form using Lemma 1. Therefore, at each time-slot h, each user $n \in \mathcal{N}$ uses the value of $e_n(h)$ and the reduced uncertainty about $\{e_n(t)\}_{t=h+1}^{H}$ to solve

$$\begin{aligned}\min_{\{\mathbf{y}_n(h)\}_{t=h}^{H}} \quad & \mathsf{p}_{n,h}^{(\mathcal{N})}\big(\mathbf{y}_n(h) \mid \tilde{l}_n(h)\big) + \sum_{t=h+1}^{H} \mathsf{f}_{n,t}\big(\mathbf{y}_n(t) \mid \tilde{l}_n(t)\big) \\ \text{s.t.} \quad & \big(\mathbf{y}_n(t)\big)_{t=h}^{H} \in \Omega_{\mathbf{y}_{n,h}}.\end{aligned} \tag{33}$$

Constraints	Parameters
$\{g_n(h) \leq g_n^{(\max)}\}_{h=1}^{H}$	$g_n^{(\max)} = 0.4$ kW
$\sum_{h=1}^{H} g_n(h) \leq \gamma_n^{(\max)}$	$\gamma_n^{(\max)} = 7.2$ kWh
$\{s_n(h) \leq \max\big(s_n^{(\max)}, c_n - q_n(h)\big)\}_{h=1}^{H}$	$s_n^{(\max)} = 0.5$ kW
	$c_n = 4$ kWh
$\{s_n(h) \geq \xi_n q_n(h-1)\}_{h=1}^{H}$	$\xi_n = \sqrt[24]{0.9}$
$q_n(0) = q_n(H)$	$q_n(0) = 1$ kWh

TABLE I
DISPATCHABLE ENERGY GENERATION AND STORAGE MODELS ADOPTED IN SECTION VI (ALSO EXTENSIVELY DESCRIBED IN [14]).

It is straightforward to observe that $\mathsf{p}_{n,h}^{(\mathcal{N})}\big(\mathbf{y}_n(h) \mid \tilde{l}_n(h)\big)$ in (31) and $\mathsf{f}_{n,h}\big(\mathbf{y}_n(h) \mid \tilde{l}_n(h)\big)$ in (32) are both convex in $\mathbf{y}_n(h)$, while $W_n(\cdot)$ is convex under the assumptions of Lemma 2. Hence, the optimization problem (33) is convex in $\big(\mathbf{y}_n(t)\big)_{t=h}^{H}$ and can be solved using efficient convex optimization techniques [33, Ch. 11].

VI. Numerical Results and Discussions

In this section, we illustrate numerically the performance of the DSM mechanisms described in Sections IV and V.

We consider a smart grid of $N = 100$ active users and $P = 900$ passive users over a day period of $H = 24$ time-slots of one hour each. With the same setup of [32], all demand-side users $n \in \mathcal{D}$ have randomly generated average energy consumption curves with daily average of $\sum_{h=1}^{24} \bar{e}_n(h) = 12$ kWh, with higher consumption during day-time hours (from 08:00 to 24:00) than during night-time hours (from 00:00 to 08:00) and reaching its peak between 16:00 and 24:00. The grid coefficients are chosen such that $\{K_h\}_{h=1}^{8} = K_{\text{night}}$ and $\{K_h\}_{h=9}^{24} = K_{\text{day}}$, with $K_{\text{day}} = 1.5K_{\text{night}}$ as in [10], [14], [15], [32], so as to obtain an initial price of 0.15 €/kWh when real-time penalties are neglected. Furthermore, we set $\{\alpha_h\}_{h=1}^{8} = 0.2$ and $\{\alpha_h\}_{h=9}^{24} = 0.9$, with $\{\beta_h = 1-\alpha_h\}_{h=1}^{24}$: this choice penalizes overconsumption during day-time hours and underconsumption during night-time hours.

We model $e_n(h)$ as a normal random variable with mean $\bar{e}_n(h)$ and standard deviation $\sigma_n(h)$, and we choose $\chi_n^{(\min)}(h)$ and $\chi_n^{(\max)}(h)$ to satisfy Theorem 1(a.2). For the sake of simplicity, we assume that all active users are subject to the same dispatchable production and storage models summarized in Table I. Here, $g_n^{(\max)}$ denotes the maximum energy production capability and $\gamma_n^{(\max)}$ represents the maximum amount of energy that user can generate during the period of analysis; as for the energy storage model, $s_n^{(\max)}$ indicates the maximum charging rate, ξ_n represents the leakage rate, c_n denotes the storage capacity, and $q_n(h)$ expresses the charge level at time-slot h, with $q_n(0)$ being the initial charge level. Furthermore,

$$\begin{aligned}\Omega_{\mathbf{y}_{n,h}} \triangleq \Big\{\big(\mathbf{y}_n(t)\big)_{t=h}^{H} \in \mathbb{R}^{2(H-h+1)} : \big(\big(g_n^\star(t)\big)_{t=1}^{h-1}, \big(g_n(t)\big)_{t=h}^{H}\big) \in \Omega_{\mathbf{g}_n}, \\ \big(\big(s_n^\star(t)\big)_{t=1}^{h-1}, \big(s_n(t)\big)_{t=h}^{H}\big) \in \Omega_{\mathbf{s}_n}, \text{ and } -l_n^{(\min)} \leq e_n(h) - g_n(h) + s_n(h) \leq l_n^{(\max)}, \forall h\Big\}\end{aligned} \tag{30}$$

This article has been accepted for publication in a future issue of this journal, but has not been fully edited. Content may change prior to final publication. Citation information: DOI 10.1109/TSP.2014.2307835, IEEE Transactions on Signal Processing

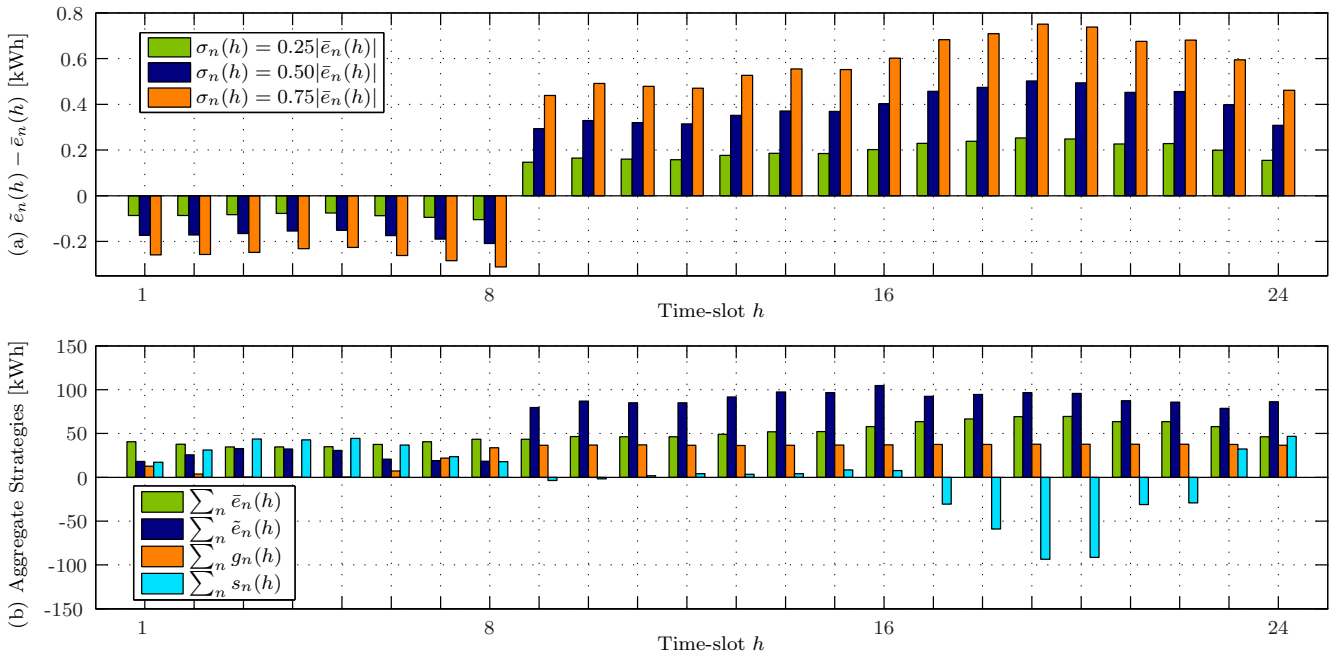

Fig. 3. Results of Algorithm 1: (a) Difference between average consumption and bid consumption for a generic user with three different $\sigma_n(h)$; (b) Aggregated average consumption and bidding, production, and storage strategies.

all dispatchable generators are characterized by the production cost function $W_n(x) = \eta_n x$, resembling a combustion engine working in the linear region, with $\eta_n = 0.039$ €/kWh.[6] Lastly, we consider Constraint 1 with $\left\{L^{(\min)}(h)\right\}_{h=1}^{H} = 385$ kWh and $\left\{L^{(\max)}(h)\right\}_{h=1}^{H} = 600$ kWh.

A. Day-Ahead DSM for Expected Cost Minimization

Here, we evaluate the performance of the Day-Ahead DSM method proposed in Section IV. For Algorithm 1, we impose $\|\mathbf{l}^{(i)} - \mathbf{l}^{(i-1)}\|_2 / \|\mathbf{l}^{(i)}\|_2 \leq 10^{-2}$ and the fulfillment of Constraint 1 as termination criteria in `(S.1)`, and $\left\{\rho^{(i)}\right\}_{i=0}^{\infty} = 1$.

Let us first analyze the results produced by Algorithm 1. Fig. 3(a) illustrates the per-slot bid net consumptions $\tilde{e}_n(h)$ with respect to the average per-slot net consumptions $\bar{e}_n(h)$ for a generic active user, using three different standard deviations. Predictably, $\tilde{e}_n(h)$ is greater than $\bar{e}_n(h)$ when $\alpha_h > \beta_h$ since the user is more likely to avoid severe penalties for surpassing the agreed load, and vice versa. Evidently, such displacement becomes greater as the standard deviation (i.e., the uncertainty) increases. Using $\sigma_n(h) = 0.75\left|\bar{e}_n(h)\right|$, Fig. 3(b) plots the aggregate bidding, production, and storage strategies obtained from Algorithm 1. As expected, the storage devices are charged at the valley of the energy cost and are discharged at peak hours; likewise, the dispatchable production is concentrated during day-time hours when the grid prices are higher.

Now, let us compare Algorithm 1 with the PDA in [32, Alg. 2], which is equivalent to the former but only considers local constraints. From Fig. 4(a), it is evident that the aggregate load produced by the PDA does not satisfy Constraint 1 during several hours (namely, $h = 3, \ldots, 5, 17, \ldots, 23$). Let us examine the resulting average expected cumulative expense: from Fig. 4(b), it is straightforward to see that active users achieve consistent savings using Algorithm 1. In particular, the average expected cumulative expense decreases from the initial value of €2.33 to €1.14 (51.1% less). However, these savings are predictably lower than those produced by [32, Alg. 2] due to the enforcement of Constraint 1. This is shown clearly by Fig. 5, which compares the convergence of the two algorithms. The PDA in [32, Alg. 2] converges after just 3 iterations; on the other hand, choosing the starting point $\mathbf{z}^{(0)} = \left(\mathbf{x}^{\star}, \boldsymbol{\lambda}^{(0)}\right)$, where $\mathbf{x}^{\star}$ is the optimal strategy profile calculated through [32, Alg. 2],[7] Algorithm 1 converges after 29 iterations. In this respect, we can observe as the average expected cumulative expense increases after about 7 iterations as a result of the imposition of Constraint 1.

Comparison with ECS Approaches. Algorithm 1 is designed to be applied specifically to the pricing model in Section III-B. Although it cannot be compared with alternative existing schemes other than [32, Alg. 2] (of which Algorithm 1 is a nontrivial generalization), it can be easily adjusted to accommodate other DSM approaches within said pricing model: this adaptability represents a remarkable feature of our framework. In particular, we extend Algorithm 1 to incorporate ECS, perhaps the most popular among the plethora of DSM techniques (see, e.g., [9], [10], [11]), into the day-ahead bidding process. In the following, we provide a comparison between ECS and DS: the former consists in shifting flexible load to off-peak hours (as discussed in Section I), whereas the latter allows to store cheap energy during off-peak hours for later use.

[6]The benefit of employing DG and DS is strictly related to the specific parameters of the adopted dispatchable source and storage device. A comparison of the impact produced by DG, DS, and a combination of the two is given in [14], [15]; furthermore, [32] provides some insight on the relative effect of the bidding strategies with respect to DG and DS strategies.

[7]This can be easily implemented by forcing the value of τ in [32, Th. 4(b.1)] and $\boldsymbol{\lambda}^{(i)} = \mathbf{0}$ until the optimal strategies without Constraint 1 are reached.

This article has been accepted for publication in a future issue of this journal, but has not been fully edited. Content may change prior to final publication. Citation information: DOI 10.1109/TSP.2014.2307835, IEEE Transactions on Signal Processing

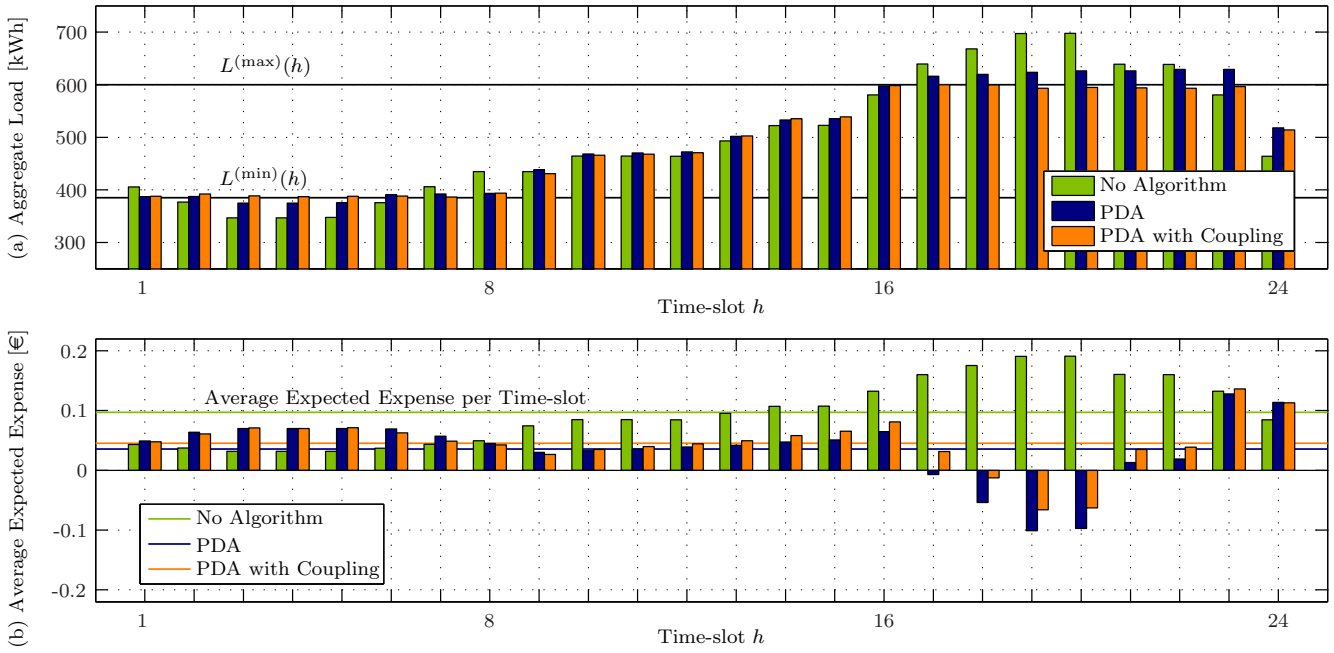

Fig. 4. Comparison between [32, Alg. 2] (PDA) and Algorithm 1 (PDA with Coupling) with $L^{(\min)} = 385$ kWh and $L^{(\max)} = 600$ kWh, $\forall h$: (a) Aggregated bid energy loads; (b) Average per-slot expected expenses.

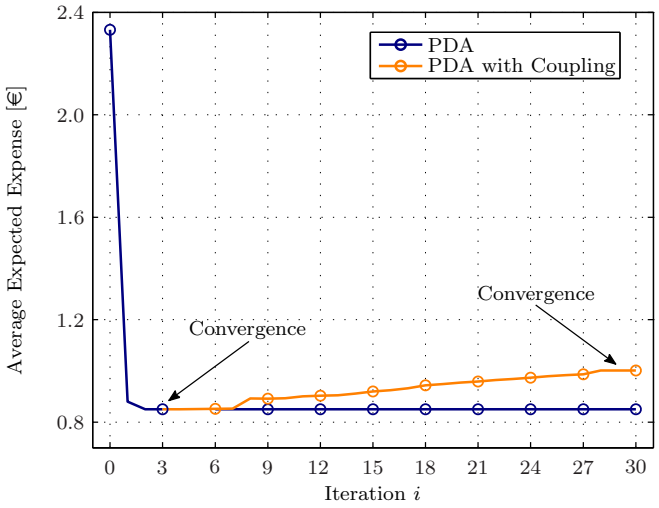

Fig. 5. Comparison between [32, Alg. 2] (PDA) and Algorithm 1 (PDA with Coupling) with $L^{(\min)} = 385$ kWh and $L^{(\max)} = 600$ kWh, $\forall h$: Convergence in terms of average expected expense.

Again, we consider $N = 100$ active users and $P = 900$ passive users with the same average consumption curves used above; furthermore, we impose Constraint 1 with $\left\{L^{(\min)}(h)\right\}_{h=1}^{H} = 415$ kWh and $\left\{L^{(\max)}(h)\right\}_{h=1}^{H} = 675$ kWh. We assume that ECS enables each active user to shift 4 kWh from peak-hours, i.e., during $h = 16, \ldots, 24$, to other time-slots; on the other hand, we consider the same setup in Table I for the energy storage (note that the amount of shiftable load and the storage device's capacity are the same). Observing Fig. 6(a), it is evident that Algorithm 1 allows to achieve similar aggregate load curves with ECS and DS. Nonetheless, from Fig. 6(b), it emerges that the expected expense obtained with ECS is slightly lower than that resulting from DS (23.6% and 16.9%, respectively, less than when no DSM approach is used). This difference can be mainly ascribed to the leakage of the storage device, which is only partially compensated by the fact that the stored energy can be sold to the grid during peak hours. On the other hand, the discomfort produced by the rescheduling of activities and the capital costs associated to controllable appliances and storage devices have not been considered here, although they are important issues to be taken into account when comparing the two methods.

B. Real-Time Adjustments of the Production and Storage Strategies

After implementing the day-ahead optimization based on Algorithm 1, we test the real-time adjustments of the production and storage strategies described in Section V. Here, the less uncertainty about the users' consumption corresponds to a reduced standard deviation with respect to that characterizing the day-ahead optimization. The standard deviation perceived by user n at each hour h for the upcoming time-slots $t = h + 1 \ldots H$ is thus modeled as $\sigma_{n,h}(t) = 0.75\sqrt{(t-h)/H}\left|\bar{e}_n(t)\right|$, with $h = 0$ corresponding to the day-ahead.

We use the Monte Carlo method and simulate 1000 normally distributed random consumption curves of a generic active user. Hence, in Fig. 7 we plot the histogram of the cumulative expenses obtained through the real-time adjustments and we compare these results with the case where the user simply follows his day-ahead production and storage strategies. In this case, the average expense decreases from €1.07 to €0.96 (i.e., 10.3% less); on the other hand, the associated variance (i.e., the risk intended as a dispersion measurement [2, Ch. 4.3.1]), decreases from 0.114 to 0.088 (i.e., 22.8% less). Observe that this procedure can be even more beneficial in a practical case, where the consumption statistics are estimated by the user and they do not accurately match the actual distribution.

This article has been accepted for publication in a future issue of this journal, but has not been fully edited. Content may change prior to final publication. Citation information: DOI 10.1109/TSP.2014.2307835, IEEE Transactions on Signal Processing

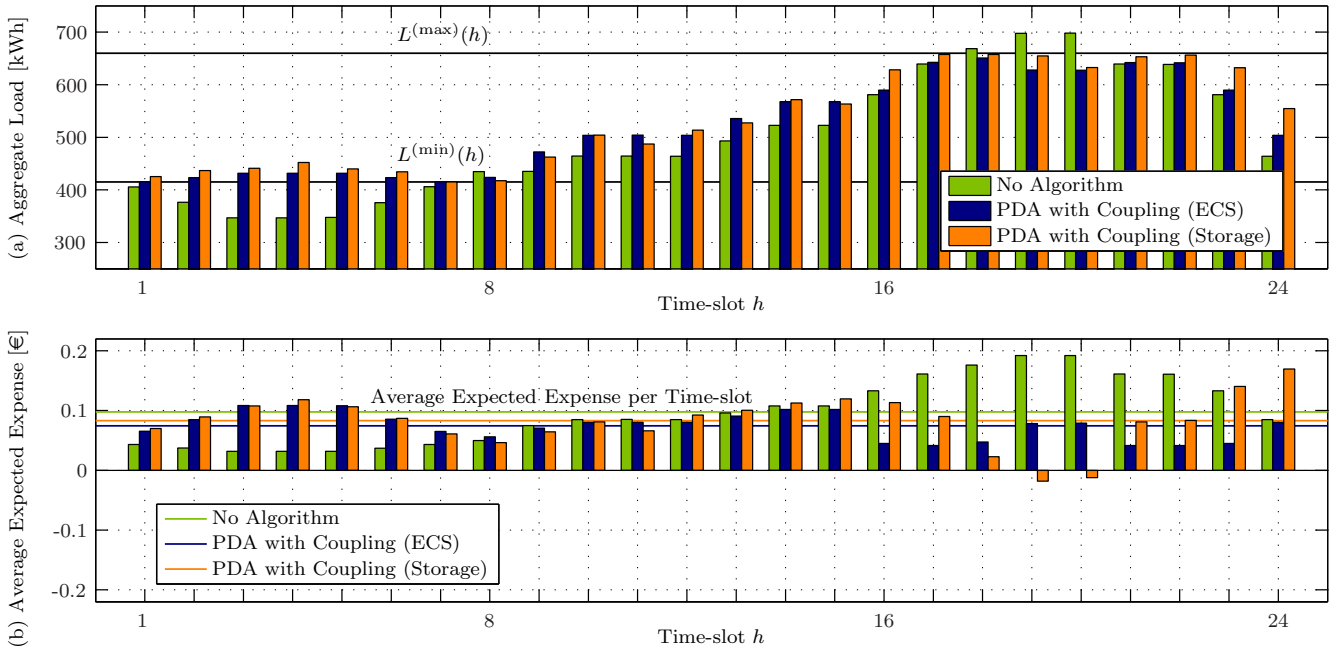

Fig. 6. Algorithm 1 (PDA with Coupling) applied to ECS and DS, with $L^{(\min)} = 415$ kWh and $L^{(\max)} = 675$ kWh, $\forall h$: (a) Aggregated bid energy loads; (b) Average per-slot expected expenses.

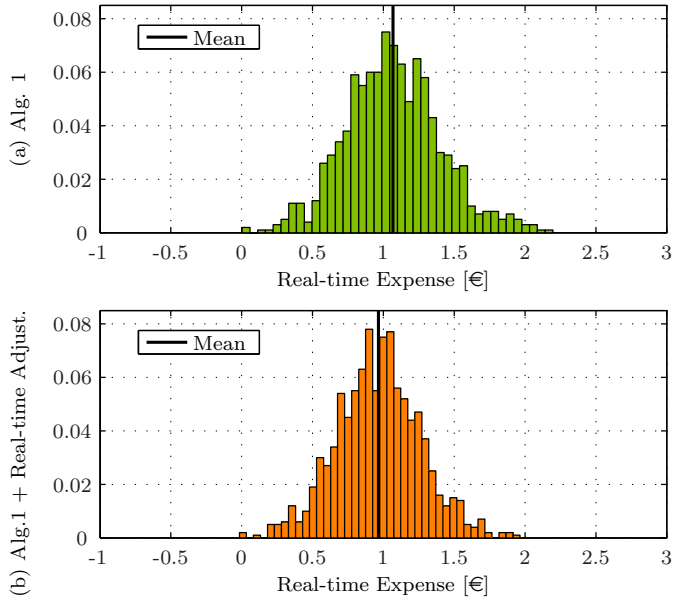

Fig. 7. Histogram of the cumulative expenses of a generic user: (a) With day-ahead strategies from Algorithm 1; (b) With additional real-time adjustments.

VII. Conclusions

In this paper, we propose a noncooperative DSM mechanism based on a pricing model with real-time penalties, which optimizes the users' bidding, production, and storage strategies at two different time granularities, i.e., day-ahead and real-time. In the day-ahead, we consider coupling constraints on the aggregate load: the grid optimization is thus formulated as a generalized Nash equilibrium problem and its main properties are studied using the general framework of variational inequality. We devise a distributed algorithm that allows to compute the variational solutions of the GNEP with limited information exchange between the central unit and the demand-side of the grid. Furthermore, in real-time, the users exploit the reduced uncertainty about their energy consumption and renewable generation to adjust their strategies, alleviating the impact of their real-time deviations with respect to the day-ahead schedule. Numerical results show that our day-ahead DSM method consistently diminishes the users' expected monetary expenses while fulfilling the global constraints. On the other hand, the real-time adjustments reduce both the average value and the variance of the user's actual monetary expense.

Appendix I
Energy Cost and Pricing Model

A. Energy Pricing for Passive Users

In order to stimulate the demand-side users to participate in the day-ahead bidding process, passive users may be penalized with respect to the active ones by paying an overprice κ_h on the purchased energy as

$$\mathsf{p}_n^{(\mathcal{P})} \triangleq \sum_{h=1}^{H} \kappa_h K_h \tilde{L}(h) l_n(h), \quad n \in \mathcal{P} \tag{34}$$

where $l_n(h) > 0$ for users $n \in \mathcal{P}$, since we assume that only active users are allowed to sell energy to the grid.

A procedure to calculate the overprice parameter κ_h is to guarantee that $\mathsf{E}\{\mathsf{p}_n^{(\mathcal{P})}\}$ is greater than the expected cumulative expense when user $n \in \mathcal{P}$ resembles an active user who simply bids his expected loads $\{\bar{l}_n(h)\}_{h=1}^{H}$. It is not difficult to show that this condition holds whenever

$$\kappa_h > 1 + \alpha_h + \beta_h. \tag{35}$$

B. Expected Cost Minimization: Proof of Lemma 1

The expected cumulative expense of active user $n \in \mathcal{N}$, with per-slot bid energy loads $\tilde{\mathbf{l}}_n$, is given by (18), where

This article has been accepted for publication in a future issue of this journal, but has not been fully edited. Content may change prior to final publication. Citation information: DOI 10.1109/TSP.2014.2307835, IEEE Transactions on Signal Processing

$\phi_{e_n(h)}\big(\mathbf{x}_n(h)\big)$ is defined in (15) and developed as shown in (36) at the bottom of the page, with $\bar{e}_n(h) = \mathsf{E}\{e_n(h)\}$. Finally, using $G_{e_n(h)}(x)$ defined in (17) and observing that

$$\int_x^\infty t f_{e_n(h)}(t)dt = \bar{e}_n(h) - G_{e_n(h)}(x) \tag{37}$$

the expression for $\phi_{e_n(h)}\big(\mathbf{x}_n(h)\big)$ in (16) readily follows. □

APPENDIX II
DAY-AHEAD DSM FOR EXPECTED COST MINIMIZATION

A. Proof of Lemma 2

The lemma follows from the application of the results in [17], [28], [29] to the specific GNEP $\mathscr{G} = \big\langle \Theta_{\mathbf{x}}, \mathbf{f} \big\rangle$ in (22). More specifically, a solution of the VI$(\Theta_{\mathbf{x}}, \mathbf{F})$ is a solution of the GNEP if the following conditions hold [17, Lem. 4.2], [28]: (a) the strategy sets $\Omega_{\mathbf{x}_n}$ in (5) are closed and convex; (b) the objective functions $\mathsf{f}_n(\mathbf{x}_n, \tilde{\mathbf{l}}_{-n})$ in (18) are convex on $\Omega_{\mathbf{x}_n}$ for any feasible $\tilde{\mathbf{l}}_{-n}$; (c) the coupling function $\mathbf{q}(\mathbf{x})$ is (jointly) convex in $\mathbf{x}$. Condition (a) is immediately satisfied if the sets $\Omega_{\mathbf{g}_n}$ and $\Omega_{\mathbf{s}_n}$ are closed and convex (note that $\Omega_{\tilde{\mathbf{e}}_n}$ in (2) is convex by definition). Likewise, condition (c) is also fulfilled for $\mathbf{q}^{(\min)}(\mathbf{x})$ and $\mathbf{q}^{(\max)}(\mathbf{x})$ defined as in (19). Hence, we only need to verify (b), i.e., the convexity of $\mathsf{f}_n(\mathbf{x}_n, \tilde{\mathbf{l}}_{-n})$.

Observe that its Hessian matrix $\mathbf{H}_{nn}(\mathbf{x})$ is obtained as

$$\mathbf{H}_{nn}(\mathbf{x}) = \mathrm{Diag}\big(\mathbf{H}_{nn}\big(\mathbf{x}(h)\big)\big)_{h=1}^{H} \tag{38}$$

with block elements $\mathbf{H}_{nn}\big(\mathbf{x}(h)\big) \triangleq \nabla^2_{\mathbf{x}_n(h)\mathbf{x}_n(h)} \mathsf{f}_n(\mathbf{x}_n, \tilde{\mathbf{l}}_{-n})$ given by (39) at the bottom of the page, $\phi_{e_n(h)}(x)$ defined in (16), and

$$\phi'_{e_n(h)}(x) \triangleq \frac{d\phi_{e_n(h)}(x)}{dx} = (\alpha_h + \beta_h) F_{e_n(h)}(x) - \alpha_h \tag{40}$$

$$\phi''_{e_n(h)}(x) \triangleq \frac{d^2\phi_{e_n(h)}(x)}{dx^2} = (\alpha_h + \beta_h) f_{e_n(h)}(x). \tag{41}$$

Hence, $\mathsf{f}_n(\mathbf{x}_n, \tilde{\mathbf{l}}_{-n})$ is convex if the partial Hessian matrices $\big\{\mathbf{H}_{nn}\big(\mathbf{x}(h)\big)\big\}_{h=1}^{H}$ are positive semidefinite. Assuming that $W_n(x)$ is convex, i.e., that $W''_n(x) \geq 0$, the smallest eigenvalue of $\mathbf{H}_{nn}(\mathbf{x}(h))$ (disregarding the null eigenvalue) is given by

$$\begin{aligned} &\frac{K_h}{2}\big(2\phi'_{e_n(h)}\big(\tilde{e}_n(h)\big) + \tilde{L}(h)\phi''_{e_n(h)}\big(\tilde{e}_n(h)\big) + 4\big) \\ &\quad - \frac{K_h}{2}\Big(\big(2\phi'_{e_n(h)}\big(\tilde{e}_n(h)\big) + \tilde{L}(h)\phi''_{e_n(h)}\big(\tilde{e}_n(h)\big) - 4\big)^2 \\ &\qquad\qquad + 2\big(2\phi'_{e_n(h)}\big(\tilde{e}_n(h)\big) + 2\big)^2\Big)^{1/2}. \end{aligned} \tag{42}$$

It thus follows that $\mathbf{H}_{nn}\big(\mathbf{x}(h)\big) \succeq 0$ if

$$2\tilde{L}(h)\phi''_{e_n(h)}\big(\tilde{e}_n(h)\big) \geq \big(\phi'_{e_n(h)}\big(\tilde{e}_n(h)\big) - 1\big)^2. \tag{43}$$

Finally, since $-\alpha_h \leq \phi'_{e_n(h)}(x) \leq \beta_h$ and $\tilde{L}(h) \geq L^{(\min)}(h)$ (see Constraint 1), (43) is satisfied whenever $\chi_n^{(\min)}$ and $\chi_n^{(\max)}$ are chosen as in Lemma 2(c). □

B. Bidding Strategy Set for Multimodal Distributions

When the pdf of the per-slot net energy consumption is multimodal, there may be multiple intervals in which Lemma 2(c) is satisfied. In this appendix, we present a heuristic method to determine the best values of $\chi_n^{(\min)}(h)$ and $\chi_n^{(\max)}(h)$, while guaranteeing the convexity of the bidding strategy sets.

Let us assume that user $n \in \mathcal{N}$ is a price taker, i.e., his load profile does not significantly affect the resulting energy prices [21]. Under this premise, the only variable term in $\mathsf{f}_n(\mathbf{x}_n, \mathbf{l}_{-n})$ in (18) is given, at each time-slot h, by $\phi_{e_n(h)}(x)$ in (16), where we have omitted the production and storage strategies. It is straightforward to see that $\phi_{e_n(h)}(x)$ is convex $\forall x$ and has a minimum at $\tilde{e}_n^{(0)}(h)$, where $\tilde{e}_n^{(0)}(h)$ is such that $F_{e_n(h)}\big(\tilde{e}_n^{(0)}(h)\big) = \alpha_h/(\alpha_h + \beta_h)$. At this point, we either have that: i) $f_{e_n(h)}\big(\tilde{e}_n^{(0)}(h)\big)$ satisfies condition (24), and $\chi_n^{(\min)}(h)$ and $\chi_n^{(\max)}(h)$ are chosen as the limit points around $\tilde{e}_n^{(0)}(h)$ that fulfill (24); or ii) $f_{e_n(h)}\big(\tilde{e}_n^{(0)}(h)\big)$ does not satisfy condition (24), and $\chi_n^{(\min)}(h)$ and $\chi_n^{(\max)}(h)$ can be found heuristically by searching intervals in the neighborhood of $\tilde{e}_n^{(0)}(h)$ such that (24) holds. In this case, when $\bar{e}_n(h) \geq 0$, it can be easily shown that $\mathsf{f}_n(\mathbf{x}_n, \mathbf{l}_{-n})$ increases for any $\tilde{e}_n(h) \geq \tilde{e}_n^{(0)}(h)$ and, hence, it is always better to chose the interval on the right-hand side of $\tilde{e}_n^{(0)}(h)$. Unfortunately, when $\bar{e}_n(h) < 0$, we do not have such clue.

C. Proof of Theorem 1

The proof of the convergence of Algorithm 1 is based on the connection between the augmented NEP (25) and VIs, and on recent results on monotone VIs [31]. Next, we first establish the connection with VIs, and then we prove the theorem.

In the setting of Lemma 2, the NEP (25) is equivalent to the partitioned VI$(\Theta_{\mathbf{x},\boldsymbol{\lambda}}, \mathbf{F}_{\boldsymbol{\lambda}})$, with $\Theta_{\mathbf{x},\boldsymbol{\lambda}} \triangleq \prod_{n=1}^{N} \Omega_{\mathbf{x}_n} \times \mathbb{R}_+^{2H}$ and $\mathbf{F}_{\boldsymbol{\lambda}}(\mathbf{x}, \boldsymbol{\lambda})$ defined as

$$\mathbf{F}_{\boldsymbol{\lambda}}(\mathbf{x}, \boldsymbol{\lambda}) \triangleq \begin{pmatrix} \mathbf{F}(\mathbf{x}) + \boldsymbol{\lambda}^{\mathrm{T}} \nabla_{\mathbf{x}} \mathbf{q}(\mathbf{x}) \\ -\mathbf{q}(\mathbf{x}) \end{pmatrix}. \tag{44}$$

Solving the NEP is then equivalent to solving the VI$(\Theta_{\mathbf{x},\boldsymbol{\lambda}}, \mathbf{F}_{\boldsymbol{\lambda}})$. Since, in the above setup, the VI$(\Theta_{\mathbf{x},\boldsymbol{\lambda}}, \mathbf{F}_{\boldsymbol{\lambda}})$ is monotone, we can hinge on distributed regularization techniques for monotone partitioned VIs [31]. More specifically, instead of solving the original VI directly, one can more easily solve, in a distributed fashion, a sequence of regularized

$$\phi_{e_n(h)}\big(\mathbf{x}_n(h)\big) = \bar{e}_n(h) - g_n(h) + s_n(h) + \alpha_h \int_{\tilde{e}_n(h)}^{\infty} \big(t - \tilde{e}_n(h)\big) f_{e_n(h)}(t)dt + \beta_h \int_{-\infty}^{\tilde{e}_n(h)} \big(\tilde{e}_n(h) - t\big) f_{e_n(h)}(t)dt \tag{36}$$

$$\mathbf{H}_{nn}\big(\mathbf{x}(h)\big) = K_h \begin{pmatrix} 2\phi'_{e_n(h)}\big(\tilde{e}_n(h)\big) + \tilde{L}(h)\phi''_{e_n(h)}\big(\tilde{e}_n(h)\big) & -\phi'_{e_n(h)}\big(\tilde{e}_n(h)\big) - 1 & \phi'_{e_n(h)}\big(\tilde{e}_n(h)\big) + 1 \\ -\phi'_{e_n(h)}\big(\tilde{e}_n(h)\big) - 1 & 2 + W''_n\big(g_n(h)\big) & -2 \\ \phi'_{e_n(h)}\big(\tilde{e}_n(h)\big) + 1 & -2 & 2 \end{pmatrix} \tag{39}$$

This article has been accepted for publication in a future issue of this journal, but has not been fully edited. Content may change prior to final publication. Citation information: DOI 10.1109/TSP.2014.2307835, IEEE Transactions on Signal Processing

strongly monotone VIs in the form $\mathrm{VI}\big(\Theta_{\mathbf{x},\boldsymbol{\lambda}}, \mathbf{F}_{\boldsymbol{\lambda}}+\tau(\mathbf{I}-\mathbf{z}^{(i)})\big)$ with $\mathbf{z}^{(i)} \triangleq (\mathbf{x}^{(i)}, \boldsymbol{\lambda}^{(i)})$. In fact, Algorithm 1 is an instance of the PDA algorithm in [32, Alg. 1] applied to the aforementioned sequence of strongly monotone regularized VIs. According to [17, Th. 4.3], its convergence is guaranteed if the following conditions are satisfied: (a) the mapping function $\mathbf{F}_{\boldsymbol{\lambda}}(\mathbf{x}, \boldsymbol{\lambda})$ in (44) is monotone on $\Theta_{\mathbf{x},\boldsymbol{\lambda}}$; (b) the regularization parameter τ is chosen such that the $(N+1)\times(N+1)$ matrix

$$\bar{\boldsymbol{\Upsilon}}_{\mathbf{F},\tau} \triangleq \begin{pmatrix} \boldsymbol{\Upsilon}_{\mathbf{F}} + \tau \mathbf{I}_N & -\mathbf{w} \\ -\mathbf{w}^{\mathrm{T}} & \tau \end{pmatrix} \tag{45}$$

is a P-matrix [17, Cor. 4.2], where $\boldsymbol{\Upsilon}_{\mathbf{F}}$ is given by

$$[\boldsymbol{\Upsilon}_{\mathbf{F}}]_{nm} \triangleq \begin{cases} \upsilon_n^{(\min)}, & \text{if } n = m \\ -\upsilon_{nm}^{(\max)}, & \text{if } n \neq m \end{cases} \tag{46}$$

$$\upsilon_n^{(\min)} \triangleq \min_{\mathbf{x}\in\Omega_{\mathbf{x}}} \lambda_{\min}\big\{\bar{\mathbf{J}}_{nn}(\mathbf{x})\big\} \tag{47}$$

$$\upsilon_{nm}^{(\max)} \triangleq \max_{\mathbf{x}\in\Omega_{\mathbf{x}}} \big\|\bar{\mathbf{J}}_{nm}(\mathbf{x})\big\| \tag{48}$$

where $\lambda_{\min}\{\cdot\}$ denotes the smallest eigenvalue of the matrix argument, $\bar{\mathbf{J}}_{nn}(\mathbf{x})$ and $\bar{\mathbf{J}}_{nm}(\mathbf{x})$ are the partial Jacobian matrices defined next in (50) and (51), respectively, and $\mathbf{w} \triangleq \big(\sup_{\mathbf{z}_n\in\Omega_{\mathbf{x}_n}} \|\nabla_{\mathbf{x}_n}\mathbf{q}_n(\mathbf{z}_n)\|_2\big)_{n=1}^N$; (c) $\rho^{(i)}$ is chosen such that $\{\rho^{(i)}\} \subset [R_m, R_M]$, with $0 < R_m < R_M < 2$.

Proof of Theorem 1(a): The mapping function $\mathbf{F}_{\boldsymbol{\lambda}}(\mathbf{x}, \boldsymbol{\lambda})$ is monotone on $\Theta_{\mathbf{x},\boldsymbol{\lambda}}$ if $\mathbf{F}(\mathbf{x})$ is so on $\Omega_{\mathbf{x}}$ [17, Prop. 4.4].

We have that $\mathbf{F}(\mathbf{x})$ is monotone on $\Omega_{\mathbf{x}}$ if the symmetric part of its Jacobian $\mathrm{J}\mathbf{F}(\mathbf{x})$ is positive semidefinite on $\Omega_{\mathbf{x}}$, i.e., $\frac{1}{2}\big(\mathrm{J}\mathbf{F}(\mathbf{x}) + \mathrm{J}\mathbf{F}^{\mathrm{T}}(\mathbf{x})\big) \succeq 0$, $\forall \mathbf{x} \in \Omega_{\mathbf{x}}$. We write the symmetric part of $\mathrm{J}\mathbf{F}(\mathbf{x})$ as

$$\bar{\mathbf{J}}(\mathbf{x}) \triangleq \frac{1}{2}\big(\mathrm{J}\mathbf{F}(\mathbf{x}) + \mathrm{J}\mathbf{F}^{\mathrm{T}}(\mathbf{x})\big) = \big(\bar{\mathbf{J}}_{nm}(\mathbf{x})\big)_{n,m=1}^N \tag{49}$$

with block elements given by

$$\bar{\mathbf{J}}_{nn}(\mathbf{x}) \triangleq \nabla^2_{\mathbf{x}_n\mathbf{x}_n} \mathsf{f}_n(\mathbf{x}_n, \tilde{\mathbf{l}}_{-n}) = \mathrm{Diag}\big(\mathbf{H}_{nn}\big(\mathbf{x}(h)\big)\big)_{h=1}^H \tag{50}$$

$$\begin{aligned} \bar{\mathbf{J}}_{nm}(\mathbf{x}) &\triangleq \frac{1}{2}\big(\nabla^2_{\mathbf{x}_n\mathbf{x}_m} \mathsf{f}_n(\mathbf{x}_n, \tilde{\mathbf{l}}_{-n}) + \nabla^2_{\mathbf{x}_m\mathbf{x}_n} \mathsf{f}_m(\mathbf{x}_m, \tilde{\mathbf{l}}_{-m})^{\mathrm{T}}\big) \\ &= \mathrm{Diag}\big(\bar{\mathbf{J}}_{nm}\big(\mathbf{x}(h)\big)\big)_{h=1}^H, \qquad n \neq m \end{aligned} \tag{51}$$

where $\mathbf{H}_{nn}\big(\mathbf{x}(h)\big)$ is given in (39) and $\bar{\mathbf{J}}_{nm}\big(\mathbf{x}(h)\big)$ is defined as in (52) at the bottom of the page. In order to guarantee that $\mathbf{z}^{\mathrm{T}}\bar{\mathbf{J}}(\mathbf{x})\mathbf{z} \geq 0, \forall \mathbf{z} \in \mathbb{R}^{3HN}$, we decompose the vector $\mathbf{z}$ as $\mathbf{z} \triangleq \big(\mathbf{z}(h)\big)_{h=1}^H$, where $\mathbb{R}^{3N} \ni \mathbf{z}(h) \triangleq \big(\mathbf{z}_n(h)\big)_{n=1}^N$ and $\mathbf{z}_n(h) \triangleq \big(z_{\tilde{e},n}(h), z_{g,n}(h), z_{s,n}(h)\big)$; then, we can write $\mathbf{z}^{\mathrm{T}}\bar{\mathbf{J}}(\mathbf{x})\mathbf{z}$ as

$$\mathbf{z}^{\mathrm{T}}\bar{\mathbf{J}}(\mathbf{x})\mathbf{z} = \sum_{h=1}^H \mathbf{z}^{\mathrm{T}}(h)\bar{\mathbf{J}}\big(\mathbf{x}(h)\big)\mathbf{z}(h) \tag{53}$$

with $\bar{\mathbf{J}}\big(\mathbf{x}(h)\big) \triangleq \big(\bar{\mathbf{J}}_{nm}\big(\mathbf{x}(h)\big)\big)_{n,m=1}^N$. Now, the proof reduces to ensuring that $\mathbf{z}(h)^{\mathrm{T}}\bar{\mathbf{J}}\big(\mathbf{x}(h)\big)\mathbf{z}(h) \geq 0$, $\forall \mathbf{z}(h) \in \mathbb{R}^{3N}$, $\forall h$.

For the sake of notation, in the following we omit the time-slot index h in the components of the auxiliary variable $\mathbf{z}(h)$. After some manipulations, it holds that

$$\begin{aligned} \big(1/K_h\big)\mathbf{z}^{\mathrm{T}}(h)\bar{\mathbf{J}}\big(\mathbf{x}(h)\big)\mathbf{z}(h) &= \Big(\sum_{n\in\mathcal{N}} z_{gs,n}\Big)^2 \\ &+ \sum_{n\in\mathcal{N}} \Big(\tilde{L}(h)\phi''_{e_n(h)}\big(\tilde{e}_n(h)\big) - \frac{1}{4}\big(\phi'_{e_n(h)}\big(\tilde{e}_n(h)\big) - 1\big)^2\Big) z^2_{\tilde{e},n} \\ &+ \Big(\sum_{n\in\mathcal{N}} \big(\phi'_{e_n(h)}\big(\tilde{e}_n(h)\big) + 1\big) z_{\tilde{e},n}\Big)\Big(\sum_{m\in\mathcal{N}} z_{gs,m}\Big) \\ &+ \Big(\sum_{n\in\mathcal{N}} \phi'_{e_n(h)}\big(\tilde{e}_n(h)\big) z_{\tilde{e},n}\Big)\Big(\sum_{m\in\mathcal{N}} z_{\tilde{e},m}\Big) \\ &+ \sum_{n\in\mathcal{N}} \Big(\frac{1}{2}\big(\phi'_{e_n(h)}\big(\tilde{e}_n(h)\big) + 1\big) z_{\tilde{e},n} + z_{gs,n}\Big)^2 \\ &+ \sum_{n\in\mathcal{N}} W''_n\big(g_n(h)\big) z^2_{g,n} \end{aligned} \tag{54}$$

where we have introduced $z_{gs,n} \triangleq z_{s,n} - z_{g,n}$. Recall that, under Lemma 2(b), $W''_n\big(g_n(h)\big) \geq 0$, $\forall n \in \mathcal{G}$, so that the term $\sum_{n\in\mathcal{N}} W''_n\big(g_n(h)\big) z^2_{g,n} \geq 0$ can be ignored.

Now, observe that $-\alpha_h \leq \phi'_{e_n(h)}(x) \leq \beta_h$, which implies $\big|\phi'_{e_n(h)}(x)\big| \leq 1$, and let us define

$$\varphi_n^{(\min)}(h) \triangleq \min_{\chi_n^{(\min)}(h)\leq x\leq\chi_n^{(\max)}(h)} \phi'_{e_n(h)}(x) \geq -\alpha_h \tag{55}$$

$$\varphi_n^{(\max)}(h) \triangleq \max_{\chi_n^{(\min)}(h)\leq x\leq\chi_n^{(\max)}(h)} \phi'_{e_n(h)}(x) \leq \beta_h \tag{56}$$

$$\varphi_n^{(\mathrm{abs})}(h) \triangleq \max\big(\big|\varphi_n^{(\min)}(h)\big|, \big|\varphi_n^{(\max)}(h)\big|\big) \tag{57}$$

and the sets $\mathcal{N}^+ \triangleq \Big\{n \;:\; z_{\tilde{e},n}\Big(\sum_{m\in\mathcal{N}} z_{gs,m}\Big) \geq 0\Big\}$ and $\mathcal{N}^- \triangleq \Big\{n : z_{\tilde{e},n}\Big(\sum_{m\in\mathcal{N}} z_{gs,m}\Big) < 0\Big\}$. Hence, it holds that

$$\begin{aligned} &\Big(\sum_{n\in\mathcal{N}} \big(\phi'_{e_n(h)}\big(\tilde{e}_n(h)\big) + 1\big) z_{\tilde{e},n}\Big)\Big(\sum_{m\in\mathcal{N}} z_{gs,m}\Big) \\ &\geq \big(\varphi_n^{(\min)}(h) + 1\big)\Big(\sum_{n\in\mathcal{N}^+} z_{\tilde{e},n}\Big)\Big|\sum_{m\in\mathcal{N}} z_{gs,m}\Big| \\ &\quad - \big(\varphi_n^{(\max)}(h) + 1\big)\Big(\sum_{n\in\mathcal{N}^-} |z_{\tilde{e},n}|\Big)\Big|\sum_{m\in\mathcal{N}} z_{\tilde{e},m}\Big| \qquad (58) \\ &\geq \big(\varphi_n^{(\min)}(h) - \varphi_n^{(\max)}(h)\big)\Big(\sum_{n\in\mathcal{N}} |z_{\tilde{e},n}|\Big)\Big|\sum_{m\in\mathcal{N}} z_{\tilde{e},m}\Big| \qquad (59) \end{aligned}$$

and

$$\begin{aligned} &\Big(\sum_{n\in\mathcal{N}} \phi'_{e_n(h)}\big(\tilde{e}_n(h)\big) z_{\tilde{e},n}\Big)\Big(\sum_{m\in\mathcal{N}} z_{\tilde{e},m}\Big) \\ &\qquad \geq -\varphi_n^{(\mathrm{abs})}(h)\Big(\sum_{n\in\mathcal{N}} |z_{\tilde{e},n}|\Big)\Big|\sum_{m\in\mathcal{N}} z_{\tilde{e},m}\Big| \qquad (60) \\ &\qquad \geq -\varphi_n^{(\mathrm{abs})}(h)\Big(\sum_{n\in\mathcal{N}} |z_{\tilde{e},n}|\Big)^2. \qquad (61) \end{aligned}$$

Now, if $\Big|\sum_{n\in\mathcal{N}} z_{gs,n}\Big| \leq \sum_{n\in\mathcal{N}} |z_{\tilde{e},n}|$, we obtain

$$\bar{\mathbf{J}}_{nm}\big(\mathbf{x}(h)\big) \triangleq \frac{K_h}{2}\begin{pmatrix} \phi'_{e_n(h)}\big(\tilde{e}_n(h)\big) + \phi'_{e_m(h)}\big(\tilde{e}_m(h)\big) & -\phi'_{e_n(h)}\big(\tilde{e}_n(h)\big) - 1 & \phi'_{e_n(h)}\big(\tilde{e}_n(h)\big) + 1 \\ -\phi'_{e_m(h)}\big(\tilde{e}_m(h)\big) - 1 & 2 & -2 \\ \phi'_{e_m(h)}\big(\tilde{e}_m(h)\big) + 1 & -2 & 2 \end{pmatrix} \tag{52}$$

This article has been accepted for publication in a future issue of this journal, but has not been fully edited. Content may change prior to final publication. Citation information: DOI 10.1109/TSP.2014.2307835, IEEE Transactions on Signal Processing

$$\begin{aligned}\big(1/K_h\big)\mathbf{z}^{\mathrm{T}}(h)\bar{\mathbf{J}}\big(\mathbf{x}(h)\big)\mathbf{z}(h) &\geq \Big(\sum_{n\in\mathcal{N}} z_{gs,n}\Big)^2 \\ &+ \sum_{n\in\mathcal{N}}\Big(\tilde{L}(h)\phi''_{e_n(h)}\big(\tilde{e}_n(h)\big) - \frac{1}{4}\big(\phi'_{e_n(h)}\big(\tilde{e}_n(h)\big)-1\big)^2 \\ &- N\big(\varphi_n^{(\mathrm{abs})}(h)+\varphi_n^{(\mathrm{max})}(h)-\varphi_n^{(\mathrm{min})}(h)\big)\Big)z_{\tilde{e},n}^2 \\ &+ \sum_{n\in\mathcal{N}}\Big(\frac{1}{2}\big(\phi'_{e_n(h)}\big(\tilde{e}_n(h)\big)+1\big)z_{\tilde{e},n}+z_{gs,n}\Big)^2. \end{aligned} \tag{62}$$

Consequently, $\mathbf{z}^{\mathrm{T}}(h)\bar{\mathbf{J}}\big(\mathbf{x}(h)\big)\mathbf{z}(h)\geq 0$ if

$$\begin{aligned}\tilde{L}(h)\phi''_{e_n(h)}\big(\tilde{e}_n(h)\big) &\geq \frac{1}{4}\big(\varphi_n^{(\mathrm{min})}(h)-1\big)^2 \\ &+ N\big(\varphi_n^{(\mathrm{abs})}(h)+\varphi_n^{(\mathrm{max})}(h)-\varphi_n^{(\mathrm{min})}(h)\big),\ \forall n\in\mathcal{N}. \end{aligned} \tag{63}$$

Otherwise, if $\Big|\sum_{n\in\mathcal{N}} z_{gs,n}\Big| > \sum_{n\in\mathcal{N}}\big|z_{\tilde{e},n}\big|$, we have that

$$\begin{aligned}\big(1/K_h\big)\mathbf{z}^{\mathrm{T}}(h)\bar{\mathbf{J}}\big(\mathbf{x}(h)\big)\mathbf{z}(h) &\geq \sum_{n\in\mathcal{N}}\Big(\tilde{L}(h)\phi''_{e_n(h)}\big(\tilde{e}_n(h)\big) \\ &- \frac{1}{4}\big(\phi'_{e_n(h)}\big(\tilde{e}_n(h)\big)-1\big)^2 - N\varphi_n^{(\mathrm{abs})}(h)\Big)z_{\tilde{e},n}^2 \\ &+ \big(1-\varphi_n^{(\mathrm{max})}(h)-\varphi_n^{(\mathrm{min})}(h)\big)\Big(\sum_{n\in\mathcal{N}} z_{gs,n}\Big)^2 \\ &+ \sum_{n\in\mathcal{N}}\Big(\frac{1}{2}\big(\phi'_{e_n(h)}\big(\tilde{e}_n(h)\big)+1\big)z_{\tilde{e},n}+z_{gs,n}\Big)^2 \end{aligned} \tag{64}$$

and, therefore, $\mathbf{z}^{\mathrm{T}}(h)\bar{\mathbf{J}}\big(\mathbf{x}(h)\big)\mathbf{z}(h)\geq 0$ if both the following conditions are fulfilled, $\forall n\in\mathcal{N}$:

$$\tilde{L}(h)\phi''_{e_n(h)}\big(\tilde{e}_n(h)\big) \geq \frac{1}{4}\big(\varphi_n^{(\mathrm{min})}(h)-1\big)^2+N\varphi_n^{(\mathrm{abs})}(h) \tag{65}$$

$$\varphi_n^{(\mathrm{max})}(h)-\varphi_n^{(\mathrm{min})}(h)\leq 1. \tag{66}$$

Note that condition (63) is more restrictive than (65) and, since $\tilde{L}(h)\geq L^{(\mathrm{min})}(h)$ (from Constraint 1), we readily obtain the lower bound in (27). On the other hand, the condition in Theorem 1(a.3) comes from substituting the definitions (55)–(57) into (66). □

Proof of Theorem 1(b): Here, we determine the value of τ that ensures the P-matrix property of $\bar{\boldsymbol{\Upsilon}}_{\mathbf{F},\tau}$ in (45).

In Appendix II-A, we have shown that, under the conditions of Lemma 2, $\mathsf{f}_n(\mathbf{x}_n,\tilde{\mathbf{l}}_{-n})$ is convex on $\Omega_{\mathbf{x}_n}$: this implies that $\bar{\mathbf{J}}_{nn}(\mathbf{x})\succeq 0$, $\forall\mathbf{x}_n\in\Omega_{\mathbf{x}_n}$ and $\forall n\in\mathcal{N}$. Hence, we can already state that $\upsilon_n^{(\mathrm{min})}\geq 0$ (c.f. (47)). Let us thus examine $\upsilon_{nm}^{(\mathrm{max})} = \max_{\mathbf{x}\in\Omega_{\mathbf{x}}}\big\|\bar{\mathbf{J}}_{nm}(\mathbf{x})\big\|$, with $\bar{\mathbf{J}}_{nm}(\mathbf{x}) = \mathrm{Diag}\big(\bar{\mathbf{J}}_{nm}\big(\mathbf{x}(h)\big)\big)_{h=1}^{H}$ and $\bar{\mathbf{J}}_{nm}\big(\mathbf{x}(h)\big)$ defined as in (52): it holds that

$$\max_{\mathbf{x}\in\Omega_{\mathbf{x}}}\big\|\bar{\mathbf{J}}_{nm}(\mathbf{x})\big\| \leq \max_h\Big(\max_{\mathbf{x}\in\Omega_{\mathbf{x}}}\lambda_{\max}\big\{\bar{\mathbf{J}}_{nm}\big(\mathbf{x}(h)\big)\big\}\Big) \tag{67}$$

where $\lambda_{\max}\{\cdot\}$ denotes the largest eigenvalue of the matrix argument. Hence, we have that

$$\begin{aligned}&\lambda_{\max}\big\{\bar{\mathbf{J}}_{nm}\big(\mathbf{x}(h)\big)\big\} \\ &= K_h\Big(1+\frac{1}{4}\Big(\phi'_{e_n(h)}\big(\tilde{e}_n(h)\big)+\phi'_{e_m(h)}\big(\tilde{e}_m(h)\big)\Big) \\ &\quad+\frac{1}{4}\Big(\phi'_{e_n(h)}\big(\tilde{e}_n(h)\big)^2+\phi'_{e_m(h)}\big(\tilde{e}_m(h)\big)^2 \\ &\quad+10\phi'_{e_n(h)}\big(\tilde{e}_n(h)\big)\phi'_{e_m(h)}\big(\tilde{e}_m(h)\big)+24\Big)^{1/2}\Big) \end{aligned} \tag{68}$$

with $\phi'_{e_n(h)}(x)$ defined in (40), and, using (56)–(57), we obtain

$$\begin{aligned}(68) &\leq K_h\Big(1+\frac{1}{4}\Big(\varphi_n^{(\mathrm{max})}(h)+\varphi_m^{(\mathrm{max})}(h)\Big)+\frac{1}{4}\Big(\varphi_n^{(\mathrm{abs})}(h)^2 \\ &\quad+\varphi_m^{(\mathrm{abs})}(h)^2+10\varphi_n^{(\mathrm{abs})}(h)\varphi_m^{(\mathrm{abs})}(h)+24\Big)^{1/2}\Big) \quad (69) \\ &\leq K_h\Big(1+\frac{\alpha_h}{2}+\frac{\sqrt{3}}{2}\big(\max(\alpha_h,\beta_h)^2+2\big)^{1/2}\Big) < 3K_h. \quad (70)\end{aligned}$$

Therefore, combining the previous results, we have that

$$\upsilon_n^{(\mathrm{min})}\geq 0 \tag{71}$$

$$\upsilon_{nm}^{(\mathrm{max})} < 3\big(\max_h K_h\big). \tag{72}$$

Now, observe that $\big(-\mathbf{q}^{(\mathrm{min})}(\mathbf{x})\big)^+ \perp \big(-\mathbf{q}^{(\mathrm{max})}(\mathbf{x})\big)^+$, where $\mathbf{a}\perp\mathbf{b}$ means $\mathbf{a}^{\mathrm{T}}\mathbf{b}=\mathbf{0}$, with $\mathbf{q}^{(\mathrm{min})}(\mathbf{x})$ and $\mathbf{q}^{(\mathrm{max})}(\mathbf{x})$ defined as in (19). Now, let us introduce $\boldsymbol{\omega}\triangleq(-\boldsymbol{\omega}^{(\mathrm{min})},\boldsymbol{\omega}^{(\mathrm{max})})\otimes\boldsymbol{\delta}$, where $\boldsymbol{\omega}^{(\mathrm{min})}$ and $\boldsymbol{\omega}^{(\mathrm{max})}$ are H-dimensional vectors with elements

$$[\boldsymbol{\omega}^{(\mathrm{min})}]_h \triangleq \begin{cases}0 & \text{if } \big[\mathbf{q}^{(\mathrm{min})}(\mathbf{x})\big]_h\leq 0\\ 1 & \text{if } \big[\mathbf{q}^{(\mathrm{min})}(\mathbf{x})\big]_h>0\end{cases} \tag{73}$$

$$[\boldsymbol{\omega}^{(\mathrm{max})}]_h \triangleq \begin{cases}0 & \text{if } \big[\mathbf{q}^{(\mathrm{max})}(\mathbf{x})\big]_h\leq 0\\ 1 & \text{if } \big[\mathbf{q}^{(\mathrm{max})}(\mathbf{x})\big]_h>0.\end{cases} \tag{74}$$

Since $\boldsymbol{\omega}^{(\mathrm{min})}\perp\boldsymbol{\omega}^{(\mathrm{max})}$, we have that $[\mathbf{w}]_n=\sqrt{\boldsymbol{\omega}^{\mathrm{T}}\boldsymbol{\omega}}\leq\sqrt{3H}$. Hence, we can state that $\bar{\boldsymbol{\Upsilon}}_{\mathbf{F},\tau}\succeq\widetilde{\boldsymbol{\Upsilon}}_{\mathbf{F},\tau}$, where

$$\big[\widetilde{\boldsymbol{\Upsilon}}_{\mathbf{F}}\big]_{nm} \triangleq \begin{cases}\tau, & \text{if } n=m\\ -3\max_h K_h, & \text{if } n\neq m \text{ and } n,m\neq N+1\\ -\sqrt{3H}, & \text{otherwise.}\end{cases} \tag{75}$$

By [17, Prop. 4.3], the matrix $\widetilde{\boldsymbol{\Upsilon}}_{\mathbf{F},\tau}$, and thus $\bar{\boldsymbol{\Upsilon}}_{\mathbf{F},\tau}$, is a P-matrix if, for some $w>0$, the following conditions hold:

$$\tau > 3(N-1)\max_h K_h + w\sqrt{3H} \tag{76}$$

$$\tau > N\frac{1}{w}\sqrt{3H}. \tag{77}$$

Evidently, the value of w that minimizes τ satisfies

$$3(N-1)\max_h K_h + w\sqrt{3H} = N\frac{1}{w}\sqrt{3H}. \tag{78}$$

and, substituting the obtained w back into (76), the value of τ in (28) follows, as stated in Theorem 1(b). □

REFERENCES

[1] M. Alizadeh, L. Xiao, W. Zhifang, A. Scaglione, and R. Melton, "Demand-side management in the smart grid: Information processing for the power switch," *IEEE Signal Process. Mag.*, vol. 29, no. 5, pp. 55–67, Sept. 2012.

[2] A. J. Conejo, M. Carrión, and J. M. Morales, *Decision making under uncertainty in electricity markets.* New York, NY, USA: Springer-Verlag Inc., 2010.

[3] H. Miao, S. Murugesan, and Z. Junshan, "Multiple timescale dispatch and scheduling for stochastic reliability in smart grids with wind generation integration," in *IEEE INFOCOM*, April 2011, pp. 461–465.

[4] A. Papalexopoulos and H. Singh, "Alternative design options for a real-time balancing market," in *IEEE Int. Conf. Power Ind. Comp. Appl. (PICA)*, May 2001, pp. 272–277.

This article has been accepted for publication in a future issue of this journal, but has not been fully edited. Content may change prior to final publication. Citation information: DOI 10.1109/TSP.2014.2307835, IEEE Transactions on Signal Processing

[5] S.-E. Fleten and E. Pettersen, "Constructing bidding curves for a price-taking retailer in the Norwegian electricity market," *IEEE Trans. Power Syst.*, vol. 20, no. 2, pp. 701–708, May 2005.

[6] W. Zhongping and F. Heng, "Bidding strategy for day-ahead and real-time markets based on newsvendor method in electricity markets," in *IEEE Int. Conf. Inf. Sci., Manag. Eng. (ISME)*, vol. 2, Aug. 2010, pp. 310–313.

[7] P. Samadi, A.-H. Mohsenian-Rad, R. Schober, V. Wong, and J. Jatskevich, "Optimal real-time pricing algorithm based on utility maximization for smart grid," in *IEEE Int. Conf. Smart Grid Comm. (SmartGridComm)*, Oct. 2010, pp. 415–420.

[8] J. Chow, W. De Mello, and K. Cheung, "Electricity market design: An integrated approach to reliability assurance," *Proc. IEEE*, vol. 93, no. 11, pp. 1956–1969, Nov. 2005.

[9] C. Chen, S. Kishore, and L. Snyder, "An innovative RTP-based residential power scheduling scheme for smart grids," in *IEEE Int. Conf. Acoust., Speech, Signal Process. (ICASSP)*, May 2011, pp. 5956–5959.

[10] A.-H. Mohsenian-Rad, V. Wong, J. Jatskevich, R. Schober, and A. Leon-Garcia, "Autonomous demand-side management based on game-theoretic energy consumption scheduling for the future smart grid," *IEEE Trans. Smart Grid*, vol. 1, no. 3, pp. 320–331, Dec. 2010.

[11] C. Ibars, M. Navarro, and L. Giupponi, "Distributed demand management in smart grid with a congestion game," in *IEEE Int. Conf. Smart Grid Comm. (SmartGridComm)*, Oct. 2010, pp. 495–500.

[12] X. Fang, S. Misra, G. Xue, and D. Yang, "Smart grid – the new and improved power grid: A survey," *IEEE Comm. Surveys Tutor.*, vol. PP, no. 99, pp. 1–37, 2011.

[13] M. Albadi and E. El-Saadany, "Demand response in electricity markets: An overview," in *IEEE Power Eng. Soc. Gen. Meet.*, June 2007, pp. 1–5.

[14] I. Atzeni, L. G. Ordóñez, G. Scutari, D. P. Palomar, and J. R. Fonollosa, "Demand-side management via distributed energy generation and storage optimization," *IEEE Trans. Smart Grid*, vol. 4, no. 2, pp. 866–876, June 2013.

[15] ——, "Noncooperative and cooperative optimization of distributed energy generation and storage in the demand-side of the smart grid," *IEEE Trans. Signal Process.*, vol. 61, no. 10, pp. 2454–2472, May 2013.

[16] A. Baillo, S. Cerisola, J. Fernandez-Lopez, and R. Bellido, "Strategic bidding in electricity spot markets under uncertainty: a roadmap," in *IEEE Power Eng. Soc. Gen. Meet.*, 2006, pp. 1–8.

[17] G. Scutari, D. P. Palomar, F. Facchinei, and J.-S. Pang, "Monotone games for cognitive radio systems," in *Distributed Decision-Making and Control*. New York, NY, USA: Springer-Verlag Inc., 2011.

[18] I. Atzeni, L. G. Ordóñez, G. Scutari, D. P. Palomar, and J. R. Fonollosa, "Cooperative day-ahead bidding strategies for demand-side expected cost minimization," in *IEEE Int. Conf. Acoust., Speech, Signal Process. (ICASSP)*, May 2013, pp. 5224–5228.

[19] F. Facchinei and J.-S. Pang, *Finite-Dimensional Variational Inequalities and Complementarity Problems*. New York, NY, USA: Springer-Verlag Inc., 2003.

[20] ——, "Nash equilibria: the variational approach," in *Convex Optimization in Signal Processing and Communication*. London, UK: Cambridge University Press, 2009, ch. 11, pp. 443–493.

[21] R. Herranz, A. Munoz San Roque, J. Villar, and F. Campos, "Optimal demand-side bidding strategies in electricity spot markets," *IEEE Trans. Power Syst.*, vol. 27, no. 3, pp. 1204–1213, Aug. 2012.

[22] P. Varaiya, F. Wu, and J. Bialek, "Smart operation of smart grid: Risk-limiting dispatch," *Proc. IEEE*, vol. 99, no. 1, pp. 40–57, Jan. 2011.

[23] J. Contreras, O. Candiles, J. de la Fuente, and T. Gomez, "Auction design in day-ahead electricity markets," *IEEE Trans. Power Syst.*, vol. 16, no. 1, pp. 88–96, Feb. 2001.

[24] S. Chan, K. Tsui, H. Wu, Y. Hou, Y.-C. Wu, and F. Wu, "Load/price forecasting and managing demand response for smart grids: Methodologies and challenges," *IEEE Signal Process. Mag.*, vol. 29, no. 5, pp. 68–85, Sept. 2012.

[25] G. Scutari, D. P. Palomar, F. Facchinei, and J.-S. Pang, "Convex optimization, game theory, and variational inequality theory," *IEEE Signal Process. Mag.*, vol. 27, no. 3, pp. 35–49, May 2010.

[26] J.-S. Pang and M. Fukushima, "Quasi-variational inequalities, generalized Nash equilibria, and multi-leader-follower games," *Comput. Manag. Sci.*, vol. 6, no. 3, pp. 373–375, Aug. 2009.

[27] K. Kubota and M. Fukushima, "Gap function approach to the generalized Nash equilibrium problem," *J. Optimiz. Theory, Appl.*, vol. 144, pp. 511–531, 2010.

[28] F. Facchinei, A. Fischer, and V. Piccialli, "On generalized Nash games and variational inequalities," *Operat. Res. Letters*, vol. 35, no. 2, pp. 159–164, 2007.

[29] P. T. Harker, "Generalized Nash games and quasi-variational inequalities," *Eur. J. Operat. Res.*, vol. 54, no. 1, pp. 81–94, 1991.

[30] F. Facchinei and C. Kanzow, "Generalized Nash equilibrium problems," *A Quart. J. Operat. Res. (4OR)*, vol. 5, no. 3, pp. 173–210, Sep. 2007.

[31] G. Scutari, F. Facchinei, J.-S. Pang, and D. P. Palomar, "Real and complex monotone communication games," *IEEE Trans. Inf. Theory*, To Appear, 2014. [Online]. Available: http://arxiv.org/pdf/1212.6235.pdf

[32] I. Atzeni, L. G. Ordóñez, G. Scutari, D. P. Palomar, and J. R. Fonollosa, "Day-ahead bidding strategies for demand-side expected cost minimization," in *IEEE Int. Conf. Smart Grid Comm. (SmartGridComm)*, Nov. 2012, pp. 91–96.

[33] S. Boyd and L. Vandenberghe, *Convex Optimization*. New York, NY, USA: Cambridge University Press, 2004.

Italo Atzeni (S'12) received the B.Sc. degree in electronic engineering and the M.Sc. degree with honors (summa cum laude) in telecommunications engineering, both from the University of Cagliari (Italy), in 2007 and 2009, respectively. Since 2011, he is the recipient of a Catalan Government Research Assistantship for the Signal Processing and Communications Group, Signal Theory and Communications Department at Universitat Politècnica de Catalunya - Barcelona Tech (Spain), where he is currently pursuing the Ph.D. degree.

He is currently involved in the CONSOLIDER-INGENIO project COMONSENS on Foundations and Methodologies for Future Communication and Sensor Networks. In 2013, he was visiting researcher in the Department of Electronic and Computer Engineering at the Hong Kong University of Science and Technology (HKUST). His current research interests are distributed algorithms, game theory and variational inequality applied to the Smart Grid.

Luis G. Ordóñez (S04, M09) received his electrical engineering and Ph.D. degrees from the Universitat Politècnica de Catalunya (UPC) - Barcelona Tech in 2003 and 2009 respectively. He conducted his Ph.D. at the Department of Signal Theory and Communications of UPC, where he now holds a postdoctoral research associate position. He had previously held several research appointments at at the Hong Kong University of Science and Technology (HKUST), Hong Kong. From 2001 to 2008 he participated in the European IST projects I-METRA, NEXWAY, and SURFACE. Currently he is involved in the CONSOLIDER-INGENIO project COMONSENS on Foundations and Methodologies for Future Communication and Sensor Networks. His research is devoted to studying the performance limits of wireless MIMO systems from the information-theoretic and communication points of view.

This article has been accepted for publication in a future issue of this journal, but has not been fully edited. Content may change prior to final publication. Citation information: DOI 10.1109/TSP.2014.2307835, IEEE Transactions on Signal Processing

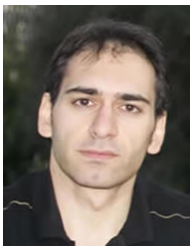

Gesualdo Scutari (S05-M06-SM'11) received the Electrical Engineering and Ph.D. degrees (both with honors) from the University of Rome La Sapienza, Rome, Italy, in 2001 and 2005, respectively.

He is an Assistant Professor in the Department of Electrical Engineering at State University of New York (SUNY) at Buffalo, Buffalo, NY. He had previously held several research appointments, namely, at University of California at Berkeley, Berkeley, CA; Hong Kong University of Science and Technology, Hong Kong; University of Rome, La Sapienza, Rome, Italy; University of Illinois at Urbana-Champaign, Urbana, IL. His primary research interests focus on theoretical and algorithmic issues related to continuous (large-scale) optimization, equilibrium programming, and their applications to signal processing, communications and networking; machine learning; smart grid; and distributed decisions.

Dr. Scutari is an Associate Editor of IEEE TRANSACTIONS ON SIGNAL PROCESSING, and he served as an Associate Editor of IEEE SIGNAL PROCESSING LETTERS. He serves on the IEEE Signal Processing Society Technical Committee on Signal Processing for Communications (SPCOM).

Dr. Scutari received the 2006 Best Student Paper Award at the International Conference on Acoustics, Speech and Signal Processing (ICASSP) 2006, the 2013 NSF Faculty Early Career Development (CAREER) Award, and the 2013 UB Young Investigator Award.

Daniel P. Palomar (S'99-M03-SM08-F'12) received the Electrical Engineering and Ph.D. degrees from the Technical University of Catalonia (UPC), Barcelona, Spain, in 1998 and 2003, respectively.

He is an Associate Professor in the Department of Electronic and Computer Engineering at the Hong Kong University of Science and Technology (HKUST), Hong Kong, which he joined in 2006. Since 2013 he is a Fellow of the Institute for Advance Study (IAS) at HKUST. He had previously held several research appointments, namely, at King's College London (KCL), London, UK; Technical University of Catalonia (UPC), Barcelona; Stanford University, Stanford, CA; Telecommunications Technological Center of Catalonia (CTTC), Barcelona; Royal Institute of Technology (KTH), Stockholm, Sweden; University of Rome La Sapienza, Rome, Italy; and Princeton University, Princeton, NJ. His current research interests include applications of convex optimization theory, game theory, and variational inequality theory to financial systems and communication systems.

Dr. Palomar is an IEEE Fellow, a recipient of a 2004/06 Fulbright Research Fellowship, the 2004 Young Author Best Paper Award by the IEEE Signal Processing Society, the 2002/03 best Ph.D. prize in Information Technologies and Communications by the Technical University of Catalonia (UPC), the 2002/03 Rosina Ribalta first prize for the Best Doctoral Thesis in Information Technologies and Communications by the Epson Foundation, and the 2004 prize for the best Doctoral Thesis in Advanced Mobile Communications by the Vodafone Foundation and COIT.

He serves as an Associate Editor of IEEE Transactions on Information Theory, and has been an Associate Editor of IEEE Transactions on Signal Processing, a Guest Editor of the IEEE Signal Processing Magazine 2010 Special Issue on "Convex Optimization for Signal Processing," the IEEE Journal on Selected Areas in Communications 2008 Special Issue on "Game Theory in Communication Systems," and the IEEE Journal on Selected Areas in Communications 2007 Special Issue on "Optimization of MIMO Transceivers for Realistic Communication Networks."

Javier R. Fonollosa (S90-M92-SM98) received the Ph.D. degree in electrical and computer engineering at Northeastern University, Boston, MA, in 1992. In 1993 he joined the Department of Signal Theory and Communications of UPC where he became Associate Professor in 1996, Professor in 2003 and Department Head from 2006 until 2010. Since March 2010 he is manager of the Communications and Electronic Technologies (TEC) area of the National Research Plan of the Ministry of Economy and Competitiveness of Spain.

He is the author of more than 100 papers in the area of signal processing and communications. Since 1995 he has played a very active participation in European Commission (EC) funded projects. In 1995 he lead UPC's participation in the projects TSUNAMI(II) and SUNBEAM that included the analysis of adaptive antennas in 2nd and 3rd generation mobile communication systems. Since January 2000 he acted as project coordinator of the projects METRA and I-METRA dedicated to the introduction of multi-antenna terminals in UMTS and Systems beyond 3G. From January 2006 to December 2008 he coordinated the EC funded project SURFACE which evaluated the performance of a generalized air interface with self-configuration capabilities. He has also been actively engaged in the National Research Plan of Spain. Since October 2006 he is project coordinator of the Type C project Fundamental bounds in Network Information Theory and since December 2008 he is project coordinator of the CONSOLIDER-INGENIO project COMONSENS on Foundations and Methodologies for Future Communication and Sensor Networks, a 5 year, 3.5 Million euro project of 135 researchers belonging to 10 universities and research centers in Spain.

In June 1995 and September 2001 he was co-chairman and organizer of the IEEE Signal Processing/ATHOS Workshop on Higher-Order Statistics held in Begur, Girona, Spain and of the IST Mobile Communications Summit 2001 held in Sitges, Barcelona, Spain. He was elected member of the Signal Processing for Communications (SPCOM) Technical Committee of the IEEE Signal Processing Society in January 1999. His research interests include many different aspects of statistical signal processing for communications and information theory. Since May 2005 he is member of the Editorial Board of the EURASIP Signal Processing Journal.